INFORMATION TO USERS

This manuscript has been reproduced from the microfilm master. UMI films the text directly from the original or copy submitted. Thus, some thesis and dissertation copies are in typewriter face, while others may be from any type of computer printer.

The quality of this reproduction is dependent upon the quality of the copy submitted. Broken or indistinct print, colored or poor quality illustrations and photographs, print bleedthrough, substandard margins, and improper alignment can adversely affect reproduction.

In the unlikely event that the author did not send UMI a complete manuscript and there are missing pages, these will be noted. Also, if unauthorized copyright material had to be removed, a note will indicate the deletion.

Oversize materials (e.g., maps, drawings, charts) are reproduced by sectioning the original, beginning at the upper left-hand corner and continuing from left to right in equal sections with small overlaps. Each original is also photographed in one exposure and is included in reduced form at the back of the book.

Photographs included in the original manuscript have been reproduced xerographically in this copy. Higher quality 6" x 9" black and white photographic prints are available for any photographs or illustrations appearing in this copy for an additional charge. Contact UMI directly to order.

UMI

A Bell & Howell Information Company
300 North Zeeb Road, Ann Arbor MI 48106-1346 USA
313/761-4700 800/521-0600

Université d'Ottawa · University of Ottawa

National Library of Canada
Acquisitions and Bibliographic Services
395 Wellington Street
Ottawa ON K1A 0N4
Canada

Bibliothèque nationale du Canada
Acquisitions et services bibliographiques
395, rue Wellington
Ottawa ON K1A 0N4
Canada

Your file Votre référence

Our file Notre référence

0-612-36735-5

Canada

I dedicate this thesis to my parents who introduced me to the field of chemistry and whom I thank for their encouragement.

Abstract

In this thesis, we present the electrochemical and spectroscopic characterization of the monolayer on a Au(111) single crystal formed by alkanethiols, dialkyldisulfides and dialkylsulfides. We found that all these organic sulfur compounds adsorb dissociatively and form a monolayer of thiolates.

We also study the monolayer formed by a cyclic sulfide, pentamethylene sulfide. We found that this sulfide forms a monolayer of an aldehyde terminated thiolate. We suggest that the sulfide is oxidatively dissociated by molecular oxygen and adsorb on the gold surface. A mechanism of this process is also described.

We use S_N2 chemistry to examine the reactivity of this cyclic sulfide. The fact that an S_N2 reaction occurs on the gold surface proves the formation of a reactive chemisorbed sulfide on the gold surface.

Acknowledgments

I thank Dr. Mario Morin, my supervisor, who introduced me to the field of electrochemical surface science. I sincerely appreciate his patience and encouragement, without which I could not have fulfilled the requirements for this thesis.

I wish to also thank Dr. Clem Kazakoff at the MS center, and Dr. Paul Mayer for his helpful discussions on the estimation of bond energies.

I wish to thank Dr. Dongfang Yang, a former research assistant in our lab, and Hongwen Chen at the MS center for their help and encouragement. I appreciate the long period of friendship with them and I believe it will last forever.

I also wish to thank all my colleagues, Hassan, Martin, Nadereh and Mark. Thanks to them all for helpful discussions.

A very special thanks to my mother, my father and my brother for their love and their support.

Table of contents

Abstract ---------- i
Acknowledgments ---------- ii
Table of contents ---------- iii

Chapter 1 Introduction

1.1 The adsorption of organic molecules on metallic surfaces ---------- 1
1.1.1 Langmuir-Blodgett (LB) layer ---------- 3
1.1.2 Self-assembled monolayer(SAM) ---------- 3
1.2 Sulfur compounds adsorbed on gold surfaces ---------- 4
References ---------- 7

Chapter 2 Experimental

2.1. Single Crystal Preparation ---------- 13
2.2. Electrochemical experiment ---------- 17
2.2.1 Cyclic voltammetry ---------- 17
2.2.2. Chronoamperometry ---------- 19
2.2.3 Electrochemical cell ---------- 20
2.2.4 Electrochemical experiment in our project ---------- 22
2.3. Infrared reflection-absorption spectroscopy (IRAS) ---------- 25
References ---------- 28

Chapter 3 Results

3.1 Dialkylsulfides ---------- 29
3.2. Pentamethylene sulfide ---------- 48
3.3. S_N2 reactions on the Au(111) surface ---------- 55
References ---------- 64

Chapter 4 Mechanism of adsorption of sulfides on Au(111)

4.1. Adsorption of symmetric dialkylsulfides on Au(111) ---------- 66
4.2. Pentamethylene sulfide adsorption on Au(111) ---------- 67
4.3. S_N2 chemistry on the Au(111) surface ---------- 70
References ---------- 74

Chapter 5 Conclusion ---------- 76

Chapter 1

Introduction

1.1 The adsorption of organic molecules on metallic surfaces

Organic molecules which form organized monolayers on metallic surfaces can be used as electrochemical sensors. The adsorption of an organic film on a metallic surface changes its electrochemical characteristics. For example, electron-transfer at an uncoated metallic electrode is comparatively nonselective. However, once an organic monolayer is adsorbed on the electrode surface, the electrochemical response depends on the ionic charge[1-1], hydrophobicity or hydrophilicity[1-2], size[1-3, 1-4, 1-5] and identity[1-6] of the electroactive species. Such modified electrodes have been used as models for studies of heterogeneous electron transfer[1-7 to 1-14], as selective membranes for electron-transfer[1-3 to 1-6] and electrical double-layers[1-15]. They can be also used as models of biological membranes[1-16] or as effective photoresists[1-17].

The two most common techniques used to form an organized monolayer on solid substrates are Langmuir-Blodgett (LB) and self-assembly (SA), shown in Fig 1.1.

1.1.1 Langmuir-Blodgett (LB) layer

The Langmuir-Blodgett was the first technique developed to deposit ordered molecular assemblies[1-18]. A LB monolayer is transferred on a substrate by contacting the substrate with a compressed organized layer spread on water or another suitable solvent [1-19 , 1-20]. Now, LB layers are widely used in areas such as sensors, corrosion, lubrication and photoresists[1-21, 1-22, 1-23].

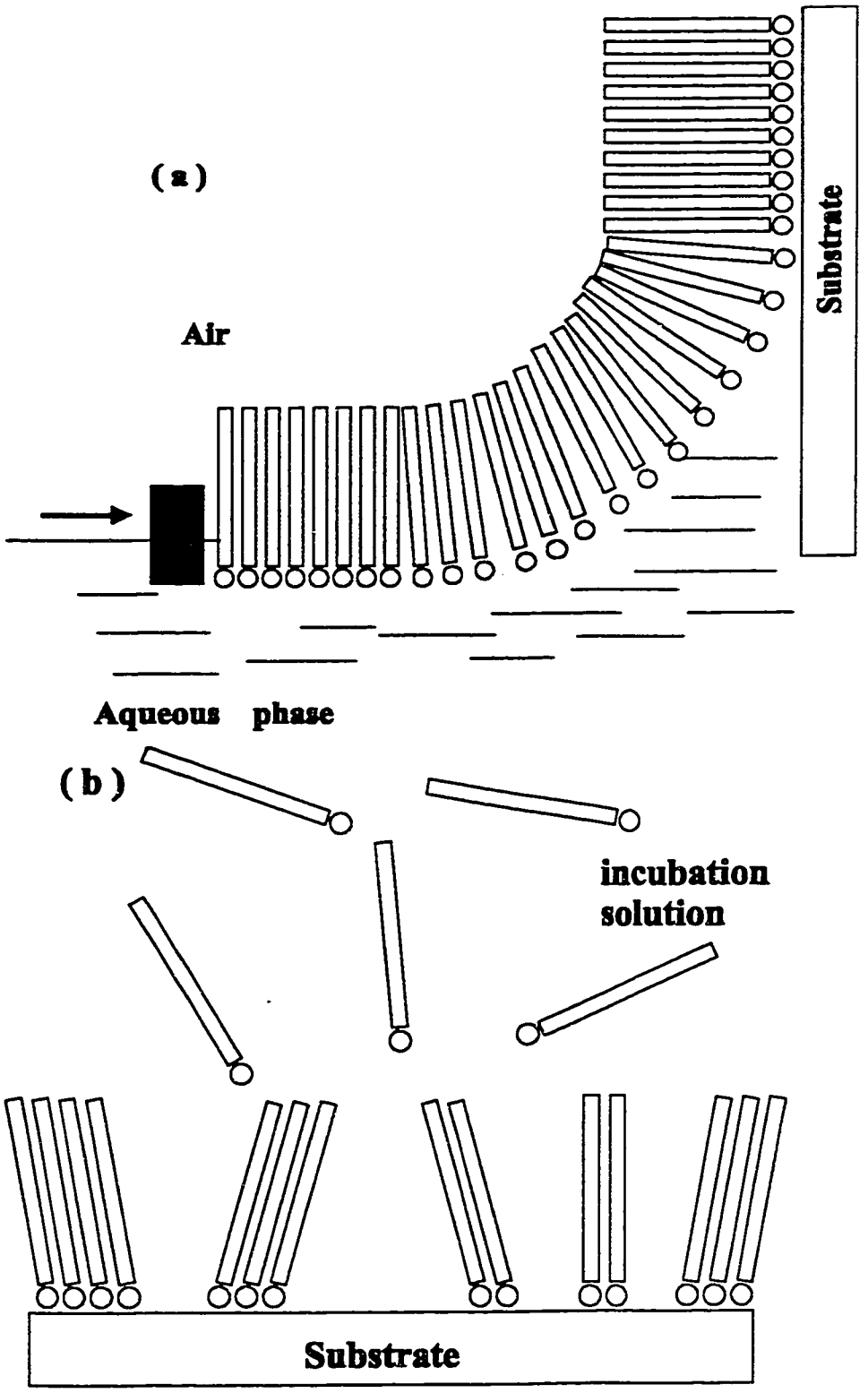

Fig 1.1 The formation of a Langmuir-Blodgett(LB) monolayer(a) and a Self-assembly monolayer(SAM)(b).

1.1.2 Self-assembled monolayer(SAM)

Self-assembled monolayers are formed by adsorbing molecules onto a substrate from a solution[1-18]. The organization and stabilization of SAM come from the chemisorption of the head group onto the substrate and favorable interactions between the adsorbates. The strength of the adsorbate-substrate interaction affects the stability, the structure and the final coverage of the monolayer. It is thus important to understand the adsorption mechanisms of these compounds.

There are several types of SAM:

1. organosilicon on hydroxylated surfaces[1-5, 1-24 to 1-28], such as SiO_2 on Si, Al_2O_3 on Al, glass, etc.
2. alcohols and amines on platinum[1-29].
3. carboxylic acids on aluminum oxide[1-30 to 1-32].
4. sulfur compounds, such as thiols, disulfides and sulfides on metallic surfaces[1-15,1-29, 1-33 to 1-41].

SAM have been studied extensively by ellipsometry, contact angle, Scanning Tunneling Microscopy(STM), Atomic Force Microscopy(AFM), Second-Harmonic Generation(SHG), helium diffraction, FTIR and various electrochemical techniques[1-18, 1-23]. In this study, cyclic voltammetry, chronoamperometry and FTIR are used(for detail see the next chapter) to characterize the SAM formed by sulfur compounds on Au(111).

1.2 Sulfur compounds adsorbed on gold surfaces.

An increased interest in SAM started when Nuzzo and Allara published a study showing that dialkyldisulfides formed an oriented monolayer on gold[1-42]. Other

sulfur compounds such as thiols and sulfides were also found to form stable monolayers on gold[1-15, 1-33 to 1-41]. Now, thiols and disulfides are widely used to form organic monolayers on gold substrates[1-23, 1-43 to 1-50]. A typical picture of an organized monolayer consists of a molecule with head and tail groups, perfectly aligned and closely packed on a smooth metal surface, as shown in Fig 1.2.

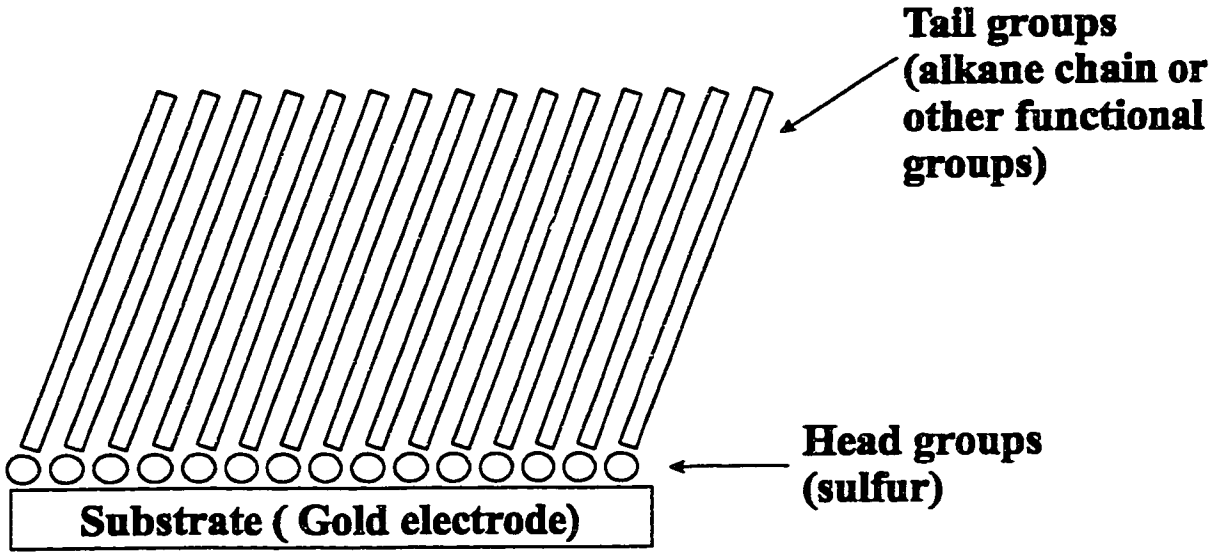

Fig 1.2 Organized monolayer of thiols adsorbed on a gold surface

Thiols and dialkyldisulfides are either strongly chemisorbed as a thiolate or as a weakly bound disulfide[1-51] on gold substrates. On a Au(111) substrate the good match between the lattice spacing and the volume of an all-trans alkane chain leads to the formation of a compact and ordered monolayer for both species[1-52,1-53]. The adsorption mechanisms of the thiols and disulfides are believed to be:

$$2\,RS\text{-}H + Au \rightarrow 2\,RS\text{-}Au + H_2 \qquad (1\text{-}1a)$$

$$2\,RS\text{-}H + Au + Oxidant \rightarrow 2\,RS\text{-}Au + H_2O \qquad (1\text{-}1b)$$

$$RS\text{-}SR + Au \rightarrow 2\,RS\text{-}Au \qquad (1\text{-}2)$$

The mechanism (1-1a) for the thiols has not been verified since no molecular hydrogen has been detected[1-18]. The adsorption of thiols on a gold substrate in an oxygen saturated solution produces peroxides, suggesting that molecular oxygen plays a role in the adsorption process and that reaction (1-1b) occurs[1-54].

The sulfur compounds commonly used to form the self-assembled monolayer on gold are thiols and disulfides. Sulfides are used less often although they offer the possibility of designing a heterogeneous organic surface[1-29]. The limited use of sulfides to form organic monolayers is due to the variation of their properties[1-29,1-55 to 1-58]. Thus alternative approaches to form a heterogeneous organic interface have been developed[1-39,1-59 to 1-62]. The origin of the variation of the properties of monolayers formed by sulfides is not clear. Contradictory conclusions about the final products of the adsorption of sulfides on a gold surface were reported. Most studies concluded that the sulfides adsorbed molecularly on the gold[1-29,1-56,1-57,1-58]. This conclusion was drawn from the frequencies of the C-H stretching modes of the chemisorbed sulfides which showed that they formed disordered monolayers. This disorder was explained by the fact that two alkane chains of a chemisorbed sulfide cannot be packed as densely as alkanethiols. Another evidence is that using TOF-SIMS(Time of Flight-Secondary Ion Mass Spectrometry), the desorption of molecular sulfide from a gold surface was observed. However, a voltammetric and spectroscopic study[1-55] indicated that sulfides dissociate on gold deposited on mica. In these studies[1-29,1-55 to 1-58], the incubation medium used was the same, undegassed ethanolic solutions of dialkylsulfides, but the gold substrates were prepared differently. The adsorption of sulfides could be influenced by the structure of the gold substrate since the dissociative adsorption often occurs at defect sites. It is possible that the discrepancies between those studies are caused by the different gold substrates. This thesis is a study of the mechanism of adsorption of sulfides on a well-defined Au(111) single crystal substrate.

References:

[1-1]: Malem, F.; Mandler, D. *Anal. Chem.* **1993**, 65, 37.

[1-2]: Wang, J.; Wu, H.; Angnes, L. *Anal. Chem.* **1993**, 65, 1893.

[1-3]: Rojas, M.T.; Koniger, R.; Stoddart, J.F.; Kaifer, A.E. *J. Am. Chem. Soc.* **1995**, 117, 336.

[1-4]: Chailapakul, O.; Crooks, R.M. *Langmuir* **1995**, 11, 1329.

[1-5]: Bilewicz, R.; Sawaguchi, T.; Chamberlain, R.V.; Majda, M. *Langmuir* **1995**, 11, 2256.

[1-6]: Steinberg, S.; Tor, Y.; Sabatani, E.; Rubinstein, I. *J. Am. Chem. Soc.* **1991**, 113, 5176.

[1-7]: Chidsey, C.E. *Science* **1991**, 251, 919.

[1-8]: Doblhofer, K.; Figura, J.; Fuhrhop, J-H. *Langmuir* **1992**, 8, 1811.

[1-9]: De Long, H.C.; Buttry, D.A. *Langmuir* **1992**, 8, 2491.

[1-10]: Rowe, G.K.; Greager, S.E. *Langmuir* **1991**, 7, 2307.

[1-11]: Lindholmsethson, B.; Orr, J.T.; Majda, M. *Langmuir* **1993**, 9, 2161.

[1-12]: Hockett, L.A.; Greager, S.E. *Langmuir* **1995**, 11, 2318.

[1-13]: Finklea, H.O.; Robinson, L.R.; Blackburn, A.; Richter, B.; Allara, D.; Bright, T. *Langmuir* **1986**, 2, 239.

[1-14]: Shimazu, K.; Ye, S.; Sato, Y.; Uosaki, K. *J. Electroanal. Chem.* **1994**, 375, 409.

[1-15]: Porter, M.D.; Bright, T.B.; Allara, D.L.; Chidsey, C.E.D. *J. Am. Chem. Soc.* **1987**, 109, 3559.

[1-16]: Lang, H.; Duschl, C.; Vogel, H. *Langmuir* **1994**, 10, 197.

[1-17]: Huang, J-Y; Dahlgren, D.A.; Hemminger, J.C. *Langmuir* **1994**, 10, 626.

[1-18]: Ulman, A. *An introduction to ultrathin organic films from Langmuir-Blodgett to self-assembly*, Academic Press; Boston, **1991**.

[1-19]: Blodgett, K.B.; Langmuir, I. *Phys. Rev.* **1937**, 51, 964.

[1-20]: Blodgett, K.B. *J. Am. Chem. Soc* **1935**, 57, 1007.

[1-21]: Swalen, J.D.; Allara, D.L.; Andrade, J.D.; Chandross, E.A.; Garoff, S.; Israelachvili, J.; McCarthy, T.J.; Murray, R.; Pease, R.F.; Rabolt, J.F.; Wynne, K.J.; Yu, H. *Langmuir* **1987**, 3, 932.

[1-22]: Fendler, J. *J. Mater. Sci* **1987**, 30, 323.

[1-23]: Finklea, H.O. in *Electroanalytical chemistry: A series of advances*, A.J.Bard and I.Rubenstein eds., Marcel Dekker, NewYork, **1997**, pp. 109

[1-24]: Sagiv, J. *J. Am. Chem. Soc.* **1980**, 102, 92.

[1-25]: Maoz, R.; Sagiv, J. *Langmuir* **1987**, 3, 1045.

[1-26]: Tillman, N.; Ulman, A.; Penner, T.L. *Langmuir* **1989**, 5, 101.

[1-27]: Netzer, L.; Sagiv, J. *J. Am. Chem. Soc.* **1983**, 105, 674.

[1-28]: Tillman, N.; Ulman, A.; Schildkraut, J.S.; Penner, T.L. *J. Am. Chem. Soc.* **1988**, 110, 6136.

[1-29]: Troughton, E.B.; Bain, C.D.; Whitesides, G.M.; Nuzzo, R.G.; Allara, D.L.; Porter, M.D. *Langumir* **1988**, 4, 365.

[1-30]: Allara, D.L.; Nuzzo, R.G. *Langmuir* **1985**, 1, 45.

[1-31]: Allara, D.L.; Nuzzo, R.G. *Langmuir* **1985**, 1, 52.

[1-32]: Ogawa, H.; Chihera, T.; Taya, K. *J. Am. Chem. Soc.* **1985**, 107, 1365.

[1-33]: Bain, C.D.; Troughton, E.B.; Tao, Y-T.; Evall, J.; Whitesides, G.M.; Nuzzo, R.G. *J. Am. Chem. Soc.* **1989**, 111, 321.

[1-34]: Nuzzo, R.G.; Dubois, L.H.; Allara, D.L. *J. Am. Chem. Soc.* **1990**, 112, 558.

[1-35]: Rubinstein, I.; Steinberg, S.; Tor, Y.; Shanzer, A.; Sagiv, J. *Nature* **1988**, 332, 426.

[1-36]: Whitesides, G.M.; Laibinis, P.E. *Langmuir* **1990**, 6, 87.

[1-37]: Chidsey, C.E.D.; Loiacono, D.N. *Langmuir* **1990**, 6, 709.

[1-38]: Chidsey, C.E.D.; Liu, G-Y; Rowntree, P.; Scoles, G. *J. Chem. Phys.* **1989**, 91, 4421.

[1-39]: Bain, C.D.; Whitesides, G.M. *J. Am. Chem. Soc.* **1989**, 111, 7164.

[1-40]: Strong, L.; Whitesides, G.M. *Langmuir* **1988**, 4, 546.

[1-41]: Nuzzo, R.G.; Fusco, F.A.; Allara, D.L. *J. Am. Chem. Soc.* **1987**, 109, 2358.

[1-42]: Nuzzo, R.G.; Allara, D.L. *J. Am. Chem. Soc.* **1983**, 105, 4481.

[1-43]: Biebuyck, H.A.; Bain, C.D.; Whitesides, G.M. *Langmuir* **1994**, 10, 1825.

[1-44]: Nuzzo, R.G.; Zegarski, B.R.; Dubois, L.H. *J. Am. Chem. Soc.* **1987**, 109, 773.

[1-45]: Karpovich, D.S.; Blanchard, G.J. *Langmuir* **1994**, 10, 3345.

[1-46]: Buck, M.; Eisert, F. *J.Electron Spec. and Rel. Phenom.* **1993**, 64/65, 159.

[1-47]: Truong, K.D.; Rowntree, P.A. *J. Phys. Chem.* **1996**, 100, 19917.

[1-48]: Tamada, K.; Hara, M.; Sasabe, H.; Knoll, W. *Langmuir* **1997**, 13, 1558.

[1-49]: Yamada, R.; Uosaki, K. *Langmuir* **1997**, 13, 5218.

[1-50]: Shimazu, K.; Yagi, I.; Sato, Y.; Uosaki, K. *Langmuir* **1992**, 8, 1385.

[1-51]: Fenter, P.; Eberhardt, A.; Eisenberg, P. *Science* **1994**, 266, 1216.

[1-52]: Camillone, N.III; Leung,T.Y.B.; Schwartz, P.; Eisenberg, P.; Scoles, G. *Langmuir* **1996**, 12, 2737.

[1-53]: Camillone, N.III; Chidsey, C.E.D.; Liu, G.Y.; Scoles, G. *J. Chem. Phys.* **1993**, 98, 4234.

[1-54]: Widrig, C.A.; Chung, C.; Porter, M.D. *J. Electroanal. Chem.* **1991**, 310, 335.

[1-55]: Zhong, C.J.; Porter, M.D. *J. Am. Chem. Soc.* **1994**, 116, 11616.

[1-56]: Zhang, M.; Anderson, M.R. *Langmuir* **1994**, 10, 2807.

[1-57]: Hagenhoff, B.; Benninghoven, A.; Spinke, J.; Liley, L.; Knoll, W. *Langmuir* **1993**, 9, 1622.

[1-58]: Beulen, M.W.; Huisman, B.H.; van der Heijden, P.A.; van Veggel F.C.J.M.; Simons, M.G.; Biemond, E.M.E.F.; de Lange, P.J.; Reinhoudt, D.N. *Langmuir* **1996**, 12, 6170.

[1-59]: Imabayashi, S.; Hobara, D.; Kakiuchi, T; Knoll, W. *Langmuir* **1997**, 13, 4502.

[1-60]: Chidsey, C.E.D.; Bertozzi, C.R.; Putvinski, T.M.; Mujsce, A.M. *J. Am. Chem. Soc.* **1990**, 112, 4301.

[1-61]: Bunding Lee, K.A.; Mowry, R.; Mclennan, G.; Finklea, H.O. *J. Electroanal. Chem.* **1988**, 246, 217.

[1-62]: Hickmann, J.J.; Laibinis, P.E.; Auerbach, D.I.; Zou, C.; Gardner, T.J.; Whitesides, G.M.; Wrighton, M.S. *Langmuir* **1992**, 8, 357.

Chapter 2

Experimental

We first describe the Au(111) single crystal preparation. Then we discuss the electrochemical techniques we used. Finally we discuss the infrared spectroscopy used in our study.

2.1. Single Crystal Preparation

a. Melting of a gold single crystal rod.

About 5 grams of pure gold (Johnson Matthey, 99.999%) was cut in small pieces and cleaned with aqua regia. It was then put into a graphite crucible which was inserted into a quartz tube previously cleaned with HNO_3. This quartz tube was inserted into the coils of an inductive furnace. The gold was melted and kept melted for about 10 to 15 minutes. Then it was slowly cooled by decreasing the furnace power at a constant rate of 50 Watts min^{-1} to allow for the formation of a single crystal. The gold rod was removed from the graphite crucible and etched in aqua regia to check if there were multiple domains on the gold rod surface. When only one domain was observed, the X-ray diffraction diagram was taken to verify if its surface was oriented in the (111) plane. The X-ray diffraction pattern of a Au(111) is shown below (Fig 2.1).

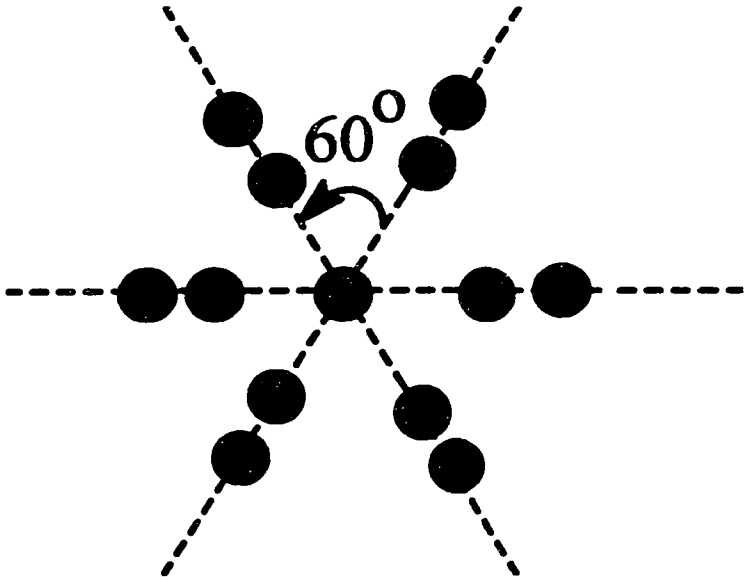

Fig 2.1 X-ray diffraction of Au(111).

b. Alignment of the single crystal.

The gold single crystal was glued on a goniometer[2-1] which allowed the adjustment of the angle of the single crystal surface. The goniometer is also used as a polishing block. The position of the gold crystal was adjusted until the (111) surface was aligned perpendicular to the axis of the goniometer with a precision of about ± 0.5°.

c. Polishing of the single crystal.

Once the crystal was aligned, a rough polish was done with 600 to 4000 grits sand paper (Struers or Buehler). A finishing polish on polishing cloths (Leco corporation) was done using three grades of diamond polishing solution (Buehler), from 6 μm down to 0.1 μm. The polishing was stopped when a mirror finished Au(111) single crystal surface was obtained.

d. Electropolishing gold single crystal surface.

The Au(111) was electropolished in a 0.1 M $HClO_4$ solution using a galvanostat in which the Au(111) was the anode and the cathode was a gold wire. A current density of 100 mA cm^{-2} was passed for about 5-10 minutes to oxidize the Au(111) surface. The oxide film was removed by immersing the Au(111) single crystal in a 10% HCl solution. These two steps were repeated 5 to 10 times.

Cyclic voltammetry (for details see next section) in a 0.1M $HClO_4$ solution between -0.2 V and 1.4 V was then used to characterize the quality of the Au(111) single crystal electrode. The Au(111) single crystal was flame annealed[2-2] in a natural gas flame, cooled in air and then quenched with deionized water (Milli-Q water system) prior to the cyclic voltammetry. The hanging meniscus method[2-3] was used to expose only the Au(111) surface. This method consists in pulling up the electrode from the electrolyte to form a meniscus so that only the surface of the gold single crystal was in contact with the solution. Then the cyclic voltammogram of the Au(111) surface was measured. Flame annealing and oxidation-reduction cycling were repeated until a typical voltammogram of a clean Au(111) surface was obtained. Such a cyclic voltammogram is shown in Fig 2.2 and it is similar to the literature[2-4].

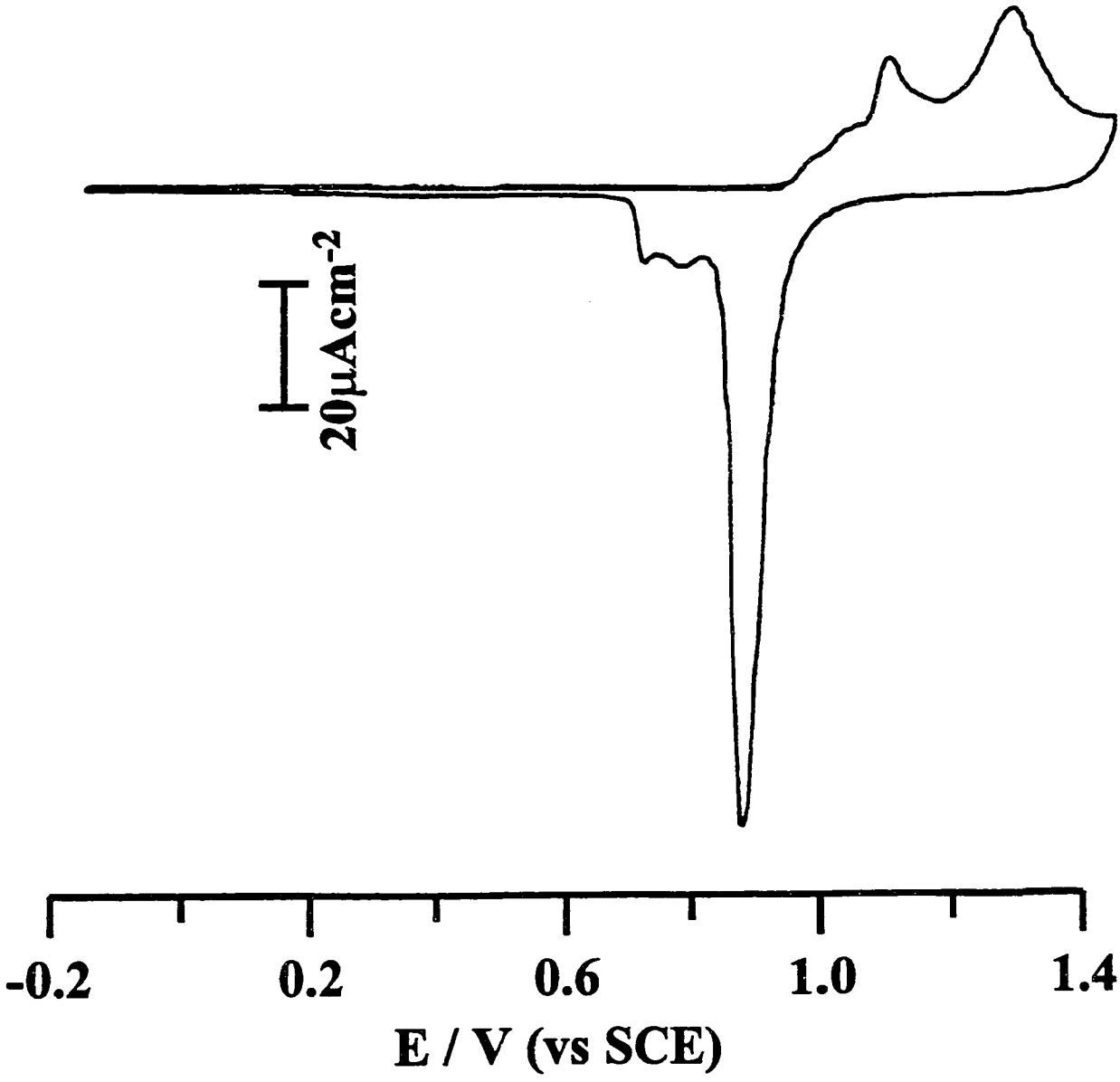

Fig 2.2 Au(111) cyclic voltammogram in 0.1 M $HClO_4$ at 20 mV s^{-1}.

2.2. Electrochemical experiment

2.2.1 Cyclic voltammetry

Cyclic voltammetry is a technique which records the current as a function of the potential applied to an electrode. The potential is varied at a constant rate as shown in Fig 2.3. The potential applied to the working electrode varies between two values. The potential begins at E_1 and is swept to a value E_2, and then reversed back to E_1. The current flowing between the working electrode and the counter electrode is measured simultaneously.

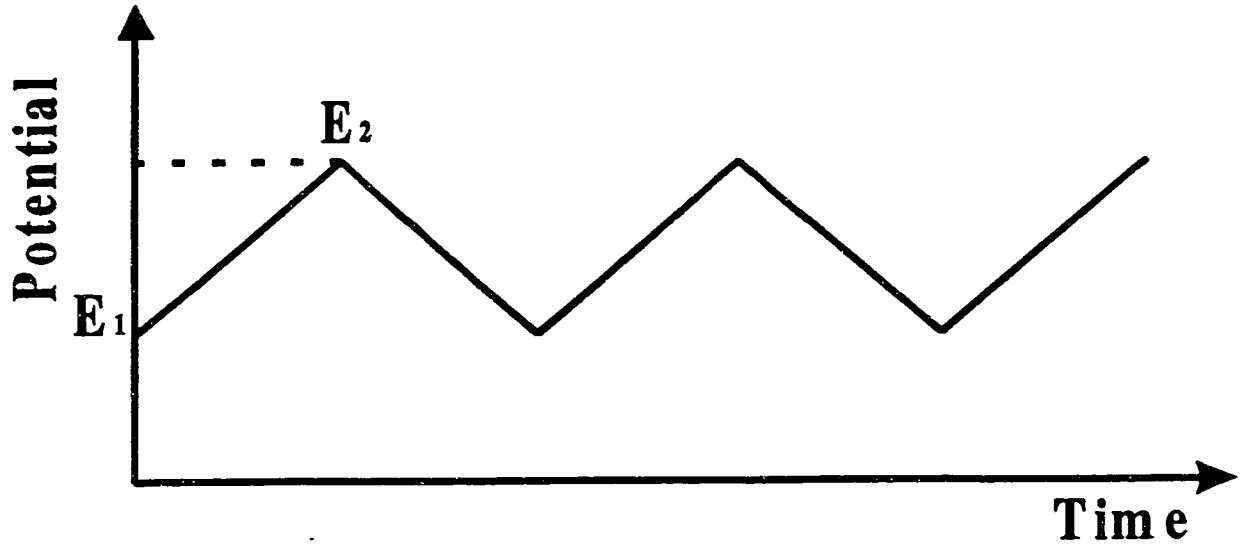

Fig 2.3 Variation of the potential applied to an electrode as a function of time in cyclic voltammetry.

The cyclic voltammogram is the i-E curve. The current is displayed on the vertical axis and the horizontal axis is the potential axis (actually it is also a time axis).

We use the three-electrode system shown in Fig 2.4 to record cyclic voltammograms. This is due to a small but non-negligible potential drop in the

solution[2-5] as shown in Fig 2.5. When the potential of the working electrode is measured against a reference electrode a voltage drop equal to iR_s will be included in the measured potential. R_s is the solution resistance between these two electrodes and i is the current. When iR_s is very small, a two-electrode system[2-6] is used because the iR_s drop can be neglected and the potential of the reference electrode remains constant. But when the iR_s potential drop gets larger, a three-electrode system must be used. A counter (also call auxiliary) electrode is introduced to the system. The current (i) then flows between the counter and the working electrode. A separated reference electrode is used to monitor the potential (E) of the working electrode. In this configuration, i is the current passing between the working electrode and the counter electrode, E is the potential applied to the working electrode relative the reference electrode potential. The absence of a significant current flowing into or out of the reference electrode ensures a stable reference potential. Even in this arrangement, a potential drop called iR_u, where R_u is the uncompensated solution resistance, still occurs. The uncompensated resistance is diminished by using a Luggin capillary located near the working electrode (see Fig 2.5).

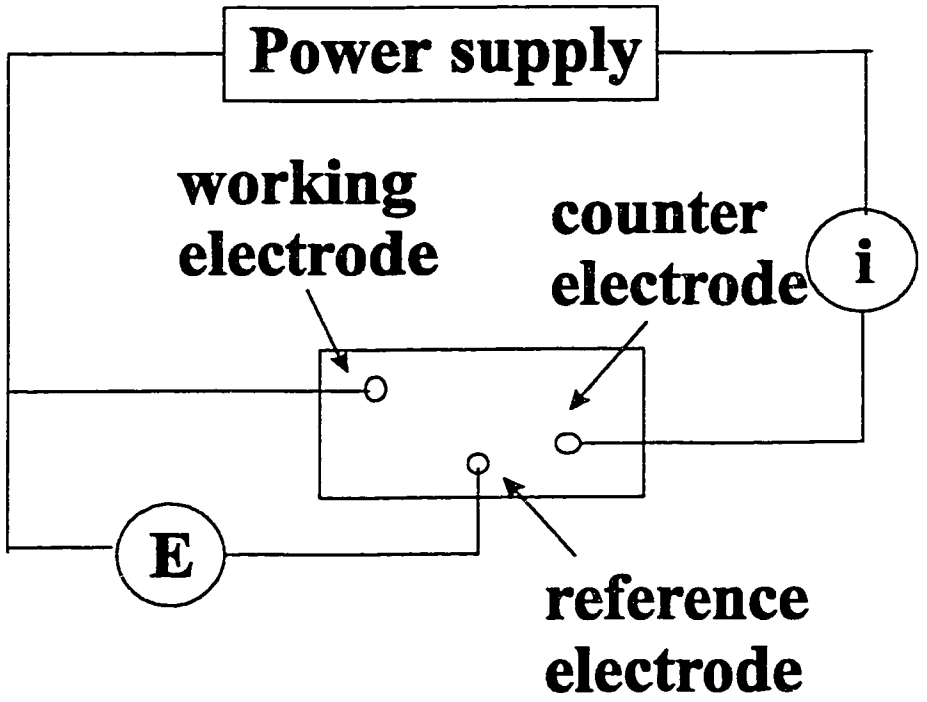

Fig 2.4 A three-electrode system.

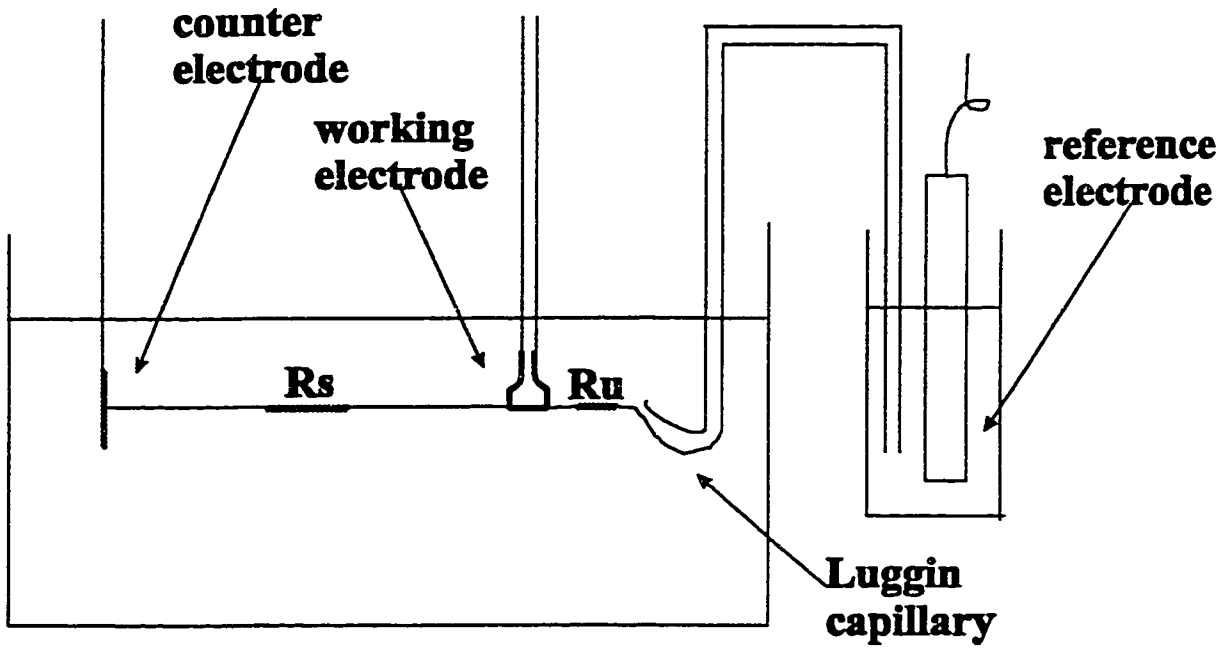

Fig 2.5 iR_s and iR_u drop in a three-electrode cell.

Cyclic voltammetry was used for two purposes. One of them is to check the Au(111) single crystal electrode quality and cleanliness. The other is to obtain information about the electrochemical properties of organic monolayers. From the shape of the reduction/oxidation current peaks, their peak potentials, their integrated charges and their double-layer capacities, the information about the coverage of molecules on the Au(111) surface and qualitative information on the strength of their bonds with the surface are obtained.

2.2.2. Chronoamperometry

Chronoamperometry consists applying a potential step to the working electrode and recording the resulting current transient (as shown in Fig 2.6). The initial potential E_1 is chosen so that there are no faradaic processes occurring. The final potential E_2 is chosen in the region where a faradaic reaction occurs. This

method is used to study the kinetics of electrochemical reactions[2-6]. In our case, chronoamperometry was used to study the mechanism of reductive desorption of thiolate monolayers on gold[2-7].

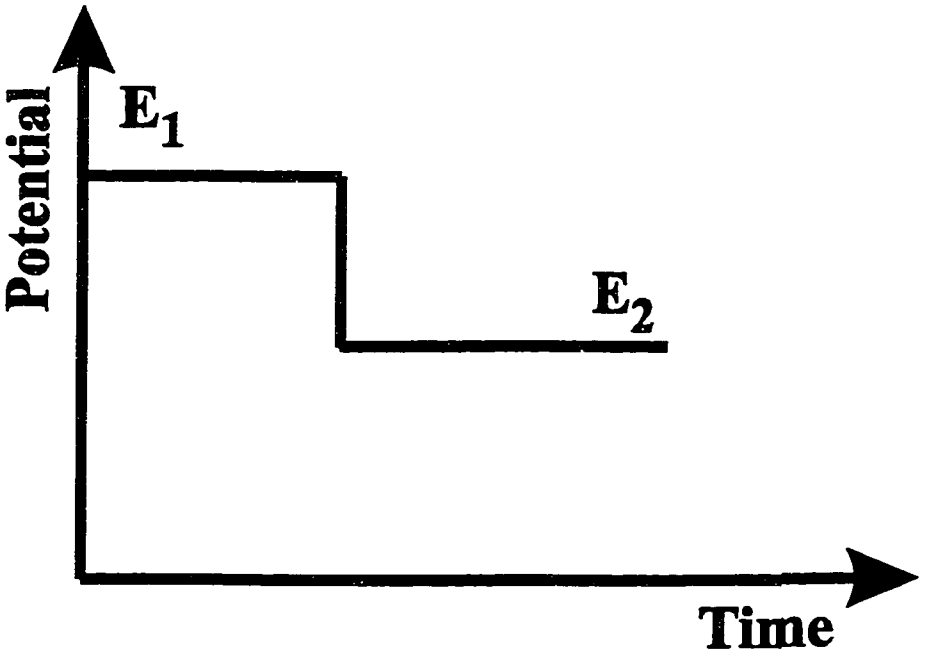

Fig 2.6 Potential-time curve in chronoamperometry

2.2.3 Electrochemical cell

All electrochemical experiments were carried out in a three-electrode cell[2-6], shown in Fig 2.7. The working electrode was a Au(111) single crystal, the counter electrode was a gold wire and the reference electrode was a saturated calomel electrode (SCE) (Fisher Scientific). The reference electrode was immersed in a bottle containing a saturated solution of KCl. The solution was in electrical contact with the electrolyte in the main electrochemical cell through a salt bridge. The salt bridge was terminated by a Luggin capillary which was close to the working electrode in order to decrease the iR_u drop. The other end of this bridge was a tube which was dipped into the saturated KCl solution in the bottle containing the reference electrode. A three way stopcock was positioned in the middle of the salt bridge.

This prevented the KCl solution from flowing from the bottle to the electrochemical cell and therefore contaminating the electrolyte solution with Cl^-. There were two inlets on the top of the electrochemical cell, one was used for degassing the solution and the other to keep a positive argon pressure. Another port on the side of the cell let the argon gas out through a bubbler. The electrochemical cell was placed inside a Faraday cage to diminish electrical and magnetic interferences.

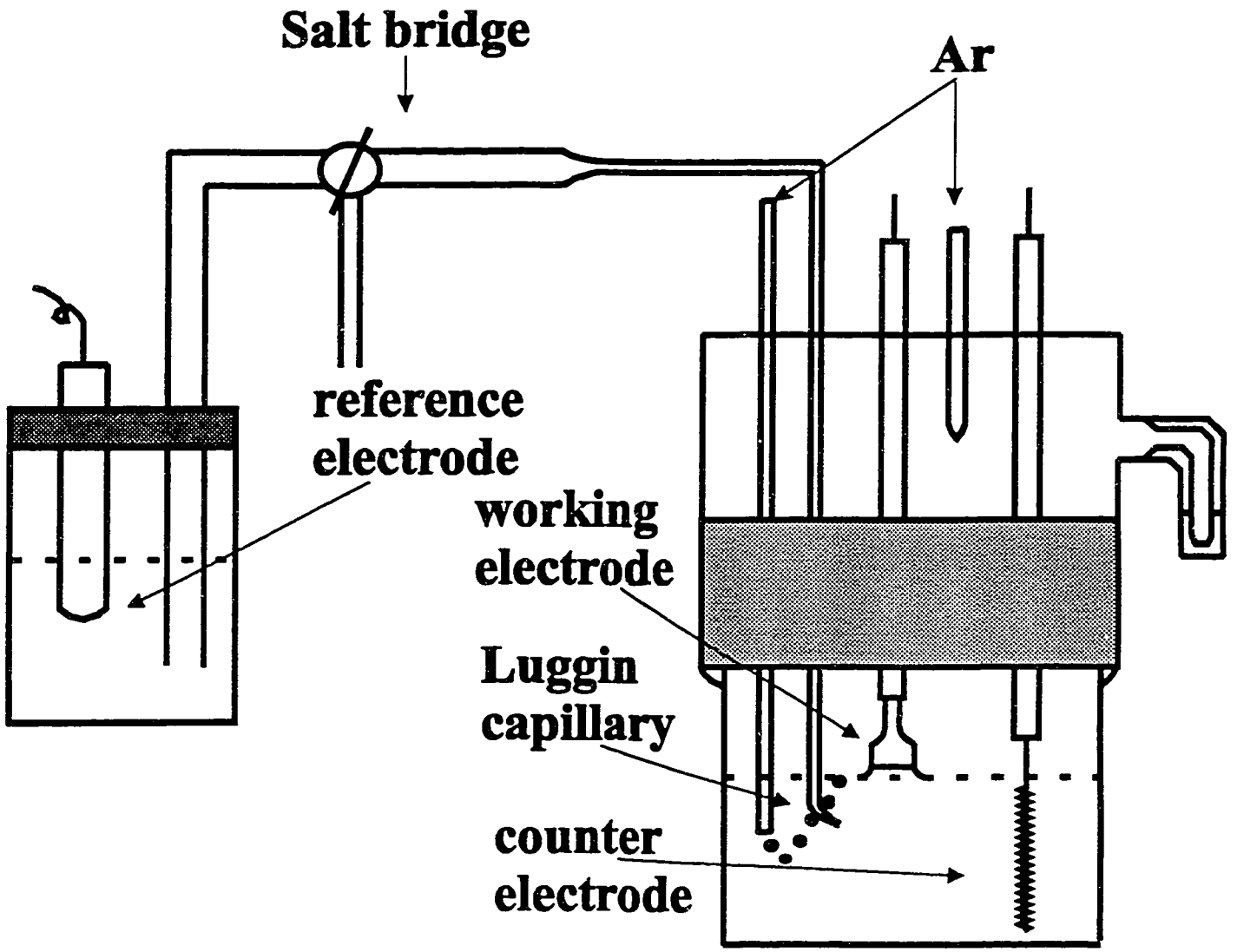

Fig 2.7 Electrochemical Cell

2.2.4 Electrochemical experiments in our project

a. Cleaning of the electrochemical cell

In order to prevent contaminations from affecting the results of the electrochemical experiment, utmost conditions of cleanliness of the electrochemical system is necessary. This is achieved by immersing the electrochemical cell into hot sulfuric acid for several hours in order to destroy organic impurities. Then the cell is rinsed with deionized water. As already mentioned in last section, the cyclic voltammogram of the Au(111) electrode in the pure supporting electrolyte was then used as a fingerprint to verify the quality of the surface of the Au(111) single crystal. This is because the current peaks related to the formation of a surface oxide seen in the cyclic voltammogram (between 0 V and 0.6 V)are characteristic of the crystallographic orientation of the gold electrode[2-4,2-6]. Cyclic voltammetry was also used to check that the supporting electrolyte was free of oxygen and of trace impurities. We thus recorded the cyclic voltammogram in the supporting electrolyte before and after the electrochemical reduction of the chemisorbed monolayer. It should be noted that gold in KOH solution is very sensitive to the presence of oxygen and organic impurities[2-8]. Alkaline conditions were chosen to push the H_2 evolution to more negative potentials. A typical cyclic voltammogram of a clean Au(111) electrode in a 0.1 M KOH solution is shown in Fig 2.8 and it is similar to the literature[2-8].

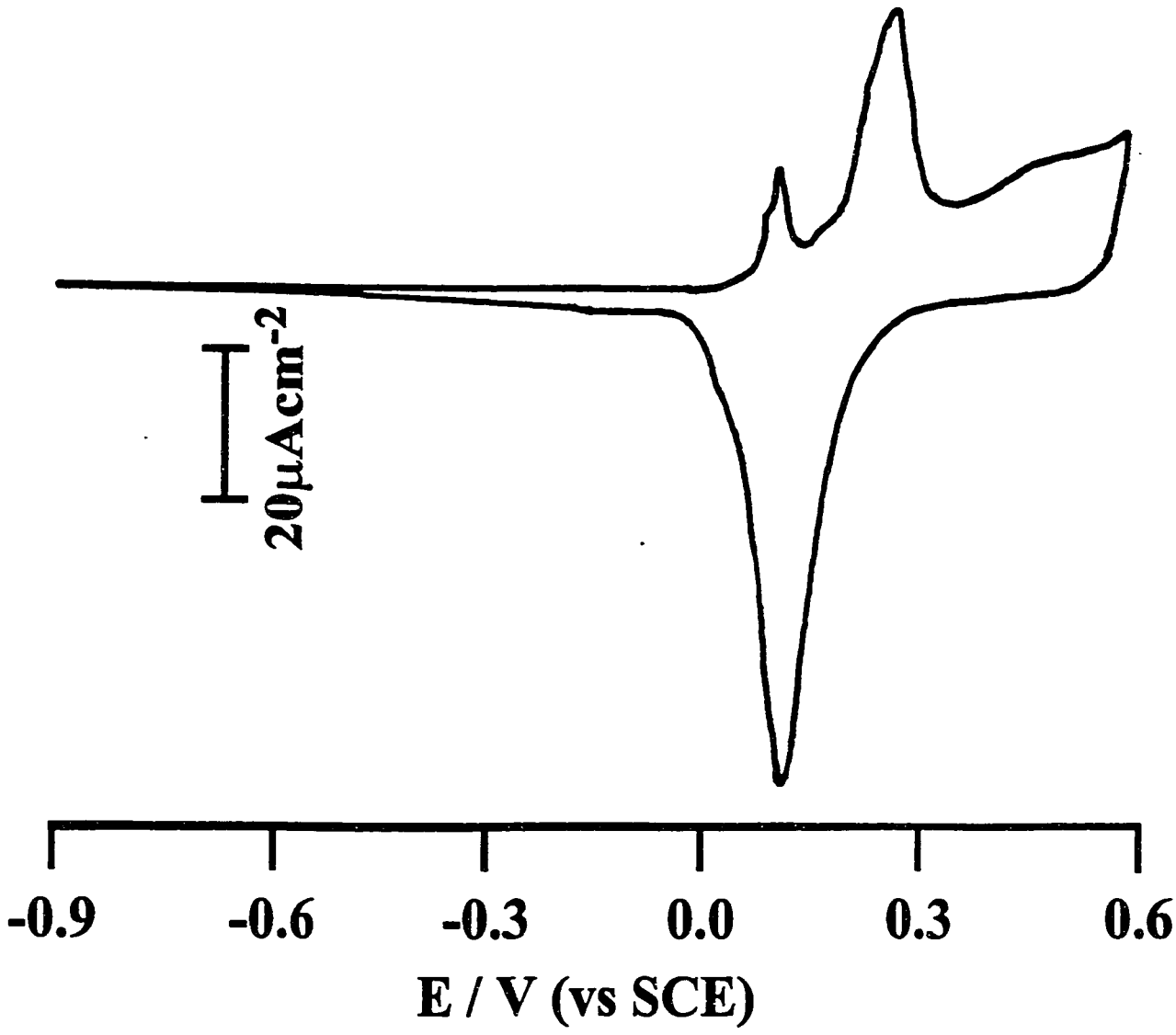

Fig 2.8 Cyclic voltammogram of Au(111) in 0.1 M KOH at 20 mV s^{-1}

b. Chemicals and electrochemical equipment.

Two Au(111) single crystals with surface areas of 0.55 cm^2 and 0.50 cm^2 were used. A three-electrode potentiostat (Pine Instrument Company, model AFRDE5 Bi-potentiostat) and a x-y recorder (Yokogawa, model 3023) were used in the cyclic voltammetry. In chronoamperometry we used a function generator (Hokoto Denko, model HB-104) and a potentiostat (EG&G, Princeton Applied Research, Model 173), a 300 MHz digital oscilloscope (Hewlett-Packard, Model 54510B) and a personal computer.

All the thiols, disulfides and sulfides were purchased from Aldrich. A careful check with GC-MS (Gas Chromatography-Mass Spectrometry) show no sulfur compounds other than the one studied. All the thiols, disulfides and sulfides were dissolved in ethanol (Omnisolv, BDH) to form 1-10 mM solution. Dimethylformamide (DMF) (Omnisolv, BDH) was also used as an incubation solvent. Ammonia (28%) was from Seastar Chemicals, Vancouver, Canada. Sodium acetate was from BDH (Analar grade). Ultrapure argon (99.999% purity, Air Product) was used to degas the electrolyte solution. Oxygen (99.6% purity, Air Product) was used to saturate the incubation solution in some experiments. The supporting electrolyte solutions were prepared with $HClO_4$ (Seastar Chemical Inc.), or KOH (Aldrich, semiconductor grade), or $KClO_4$ (Aldrich, recrystallized twice from Milli-Q water) and deionized distilled water (Milli-Q system).

c. Monolayer deposition and cyclic voltammetry.

The organic monolayer was obtained by immersing the clean Au(111) electrode in the thiol (or disulfide or sulfide) solution for a period of 30 minutes to one hour. The electrode was then removed from the thiol solution, rinsed with ethanol and Milli-Q water to removed physisorbed layers. It was immediately

transferred to the electrochemical cell and a hanging meniscus was formed. The cyclic voltammogram was recorded within one minute. In all cases, the potential of the electrode was initially scanned in the negative and then in the reverse direction. The range of potentials was limited to the region where there is no hydrogen or oxygen evolution occurring. The potential limits were -1.2 V and 0 V.

d. Chronoamperometry.

E_1 was chosen to be -0.3 V, where no reductive desorption occurs and the thiolate coated Au(111) electrode surface is stable. E_2 was chosen based on the cyclic voltammogram of the sulfur compound studied.

2.3. Infrared reflection-absorption spectroscopy (IRAS)

IR spectroscopy allows the identification of functional groups. It also proved to be a useful tool in the study of the structure and orientation of organic monolayers[2-9]. In our IRAS experiments, an infrared beam was reflected from a monolayer covered Au(111) surface and the reflectance spectrum was recorded. A second spectrum was taken under the same conditions except that there was no monolayer on the Au(111). The absorbance spectrum is then calculated using $A = -\log (I / I_0)$, where I and I_0 are the reflection intensities of the monolayer coated and clean Au(111) surfaces respectively.

The selection rule[2-10,2-11] in reflection-absorption FTIR spectroscopy is that only the transition dipoles or the component of transition dipoles perpendicular to the metal surface can be excited. Thus large angles of incidence and p-polarized light are used to maximize the intensity of the electric field perpendicular to the surface. This selection rule is based on the fact that only p-polarized infrared radiation can excite a vibrational mode of an adsorbate on a metallic surface. When the infrared light is

reflected from a metal surface, as shown in Fig 2.9, s-polarized radiation (the electric field is polarized perpendicular to the plane of incidence) undergo a phase shift of 180^0 at all angles of incidence. The incident and reflected waves cancel at the surface. However p-polarized radiation (the electric field is polarized parallel to the plane of incidence) is combined with its mirror dipole and the electric field is doubled in intensity.

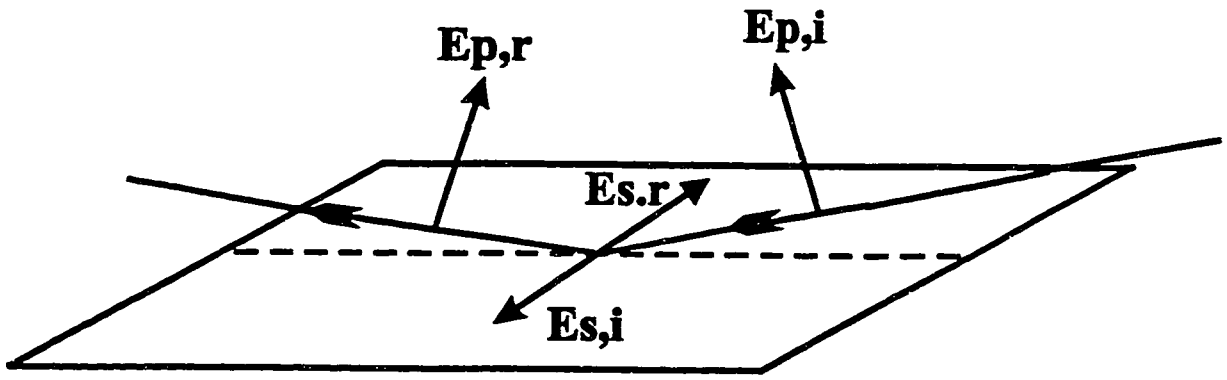

Fig 2.9 The electric field of s-polarized and p-polarized light in the incident and reflected beams on the metal surface

This gives us the possibility to obtain information about the orientation of molecular species at the interface. For example, the intensity of the methylene vibrational modes in the spectra is a function of the tilt angle of the alkyl chain relative to the metal surface, as shown in Fig 2.10 (ν_a: asymmetric -CH stretching mode transition dipole moment; ν_s: symmetric -CH stretching mode transition dipole moment).

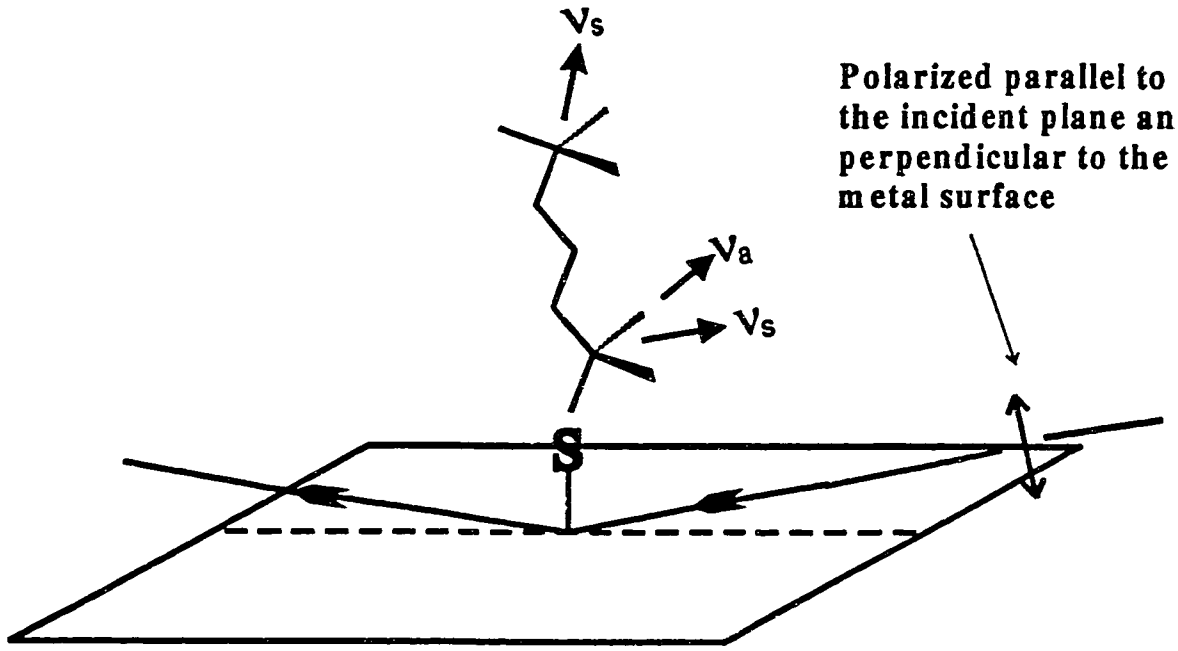

Fig 2.10 Schematic diagram of IRAS experiment

IRAS set-up:

A nitrogen-purged Nicolet Magna-IR 550 spectrometer was used. An angle of 80^{o} between the surface normal and the beam direction was used as shown in Fig 2.11. Because the amount of light absorbed by a monolayer of organic molecules is very small(10^{-3} to 10^{-4} in absorbance units), 1000 scans with a resolution of 2 cm^{-1} must be averaged to increase the signal/noise ratio in the spectra.

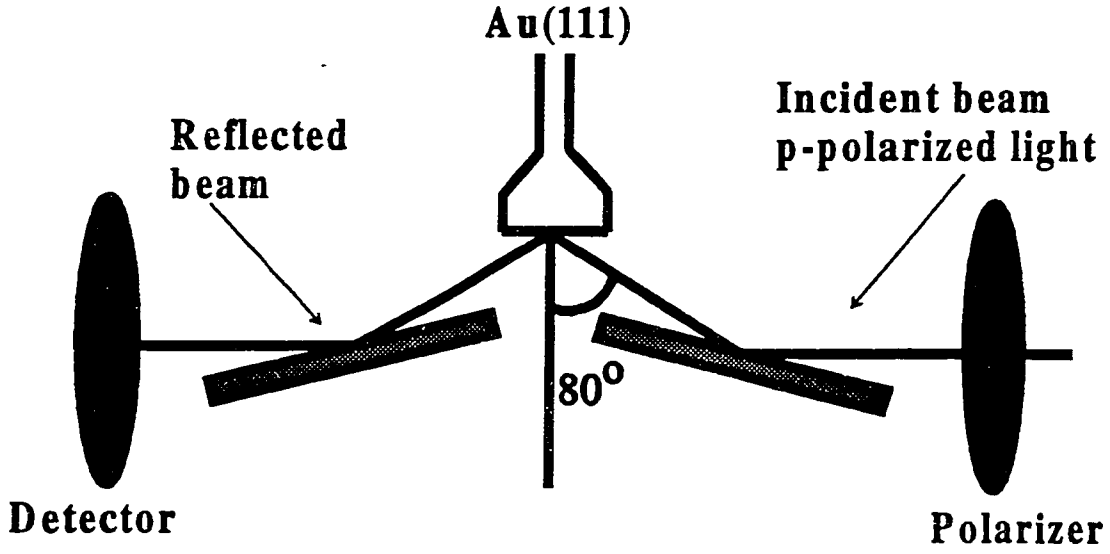

Fig 2.11 Ex-situ IR experimental set-up

References:

[2-1]: E.Revesz, M.Sc. Thesis, University of Ottawa, **1996.**

[2-2]: Clavilier, J.; Faure, R.; Guinet, G.; Durand, R. *J. Electroanal. Chem.* **1980**, 107, 205.

[2-3]: Dickertmann, D.; Koppitz, F.D.; Schultz, J.W. *Electrochimica Acta* **1976**, 12, 967.

[2-4]: Angerstein-Kozlowska, H.; Conway, B.E.; Hamelin, A.; Stoicoviciu, L. *J. Electroanal. Chem.* **1987**, 228, 429.

[2-5]: Greef, R.; Peat, R.; Peter, L.M.; Pletcher, D.; Robinson *Instrumental Methods in Electrochemistry* Ellis Horwood Limited, **1985.**

[2-6]: Bard, A.J.; Faulkner, L.R. *Electrochemical Methods- Fundamentals and Applications* John Wiley & Sons, Inc. **1980.**

[2-7]: Yang, D-F; Morin, M. *J. Electroanal. Chem.* **1997**, 429, 1.

[2-8]: Hamelin, A.; Sottomayor, M.J.; Silva, F.; Chang, S-C; Weaver, M.J. *J. Electroanal. Chem.* **1990**, 295, 291.

[2-9]: Nuzzo, R.G.; Allara, D.L. *J. Am. Chem. Soc.* **1983,** 105, 4481.

[2-10]: Ashley, K.; Pons, S. *Chem. Rev.* **1988**, 88, 673.

[2-11]: Greenler, R.G. *J. Chem. Phys.* **1966**, 44, 310.

Chapter 3

Results

In this chapter, we present the electrochemical and spectroscopic characterization of the monolayers formed by thiols, disulfides and sulfides on Au(111). They are divided into three sections. In the first section, we present the results of alkanethiols', alkyldisulfides' and alkylsulfides' electrochemical and spectroscopic properties. In the second section we present the results of a cyclic sulfide monolayer, pentamethylene sulfide, adsorbed on Au(111). In the last section, we use S_N2 chemistry to study the reactivity of this cyclic sulfide.

3.1 Dialkylsulfides

As mentioned in Chapter 1, there are two suggestions[3-1 to 3-5] for the adsorbed product formed by sulfides on a gold surface. They are the molecular or the dissociative adsorption of sulfides. In order to identify if the adsorption of sulfide is molecular or dissociative, the electrochemical and spectroscopic characteristics of a series of alkylsulfides are compared with those of thiols which have the same chain length.

At first, we did a comparison of disulfides and thiols to confirm that they form identical monolayers on Au(111) as previously reported[3-6,3-7]. Hexadecanethiol and hexadecyldisulfide were used for this purpose. The cyclic voltammogram of hexadecanethiol in Fig 3.1a shows a sharp reductive peak at -1.12 V, and a shoulder peak at -1.16 V. When the potential is swept back in the positive direction, two

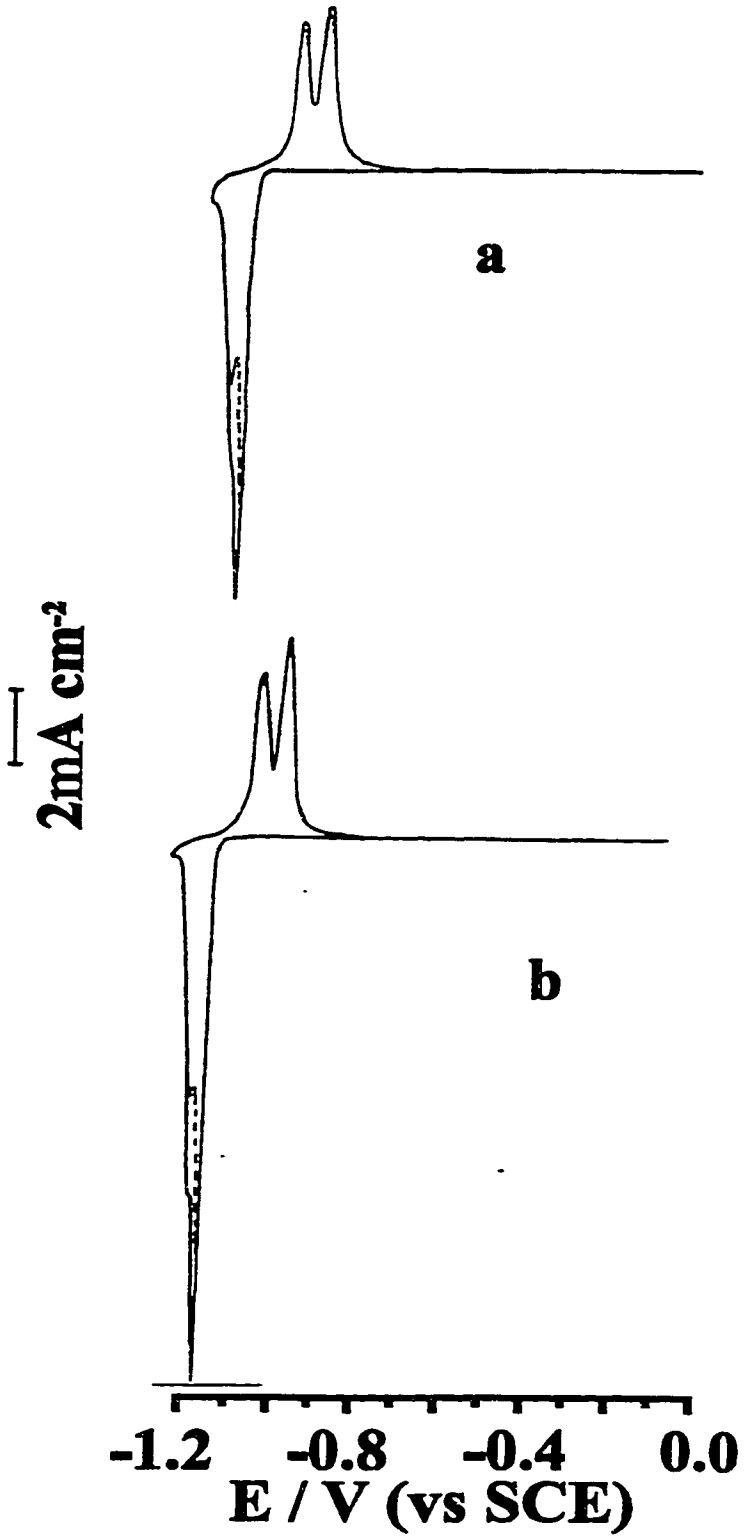

Fig 3.1 Cyclic voltammograms of (a) hexadecanethiol, (b) hexadecyldisulfide chemisorbed on Au(111) in 0.1 M KOH with a scan rate of 10 mV s^{-1}.

separate oxidative readsorption peaks appear. The first one is at -0.98 V, the other one is at -0.91 V. The cyclic voltammogram of hexadecyldisulfide in Fig 3.1b is identical to the previous one (Fig 3.1a). The vibrational spectra of the C-H stretching modes of hexadecanethiol and hexadecyldisulfide (shown in Fig 3.2a and 3.2b) are identical. They have five peaks (see Table 3.1). There is an asymmetric methyl C-H stretching mode located at 2962 cm^{-1}, a symmetric methyl stretching mode located at 2878 cm^{-1}, and its Fermi resonance mode shows a shoulder peak at 2935 cm^{-1}. The methylene symmetric and asymmetric stretch modes are located at 2850 and 2919 cm^{-1} respectively. Thus these two different sulfur compounds adsorbed on the gold surface to form identical monolayers. Because the disulfide and thiol formed the same final product, a thiolate, we just use the monolayer formed by the thiols to compare with the monolayer formed by dialkylsulfides.

The spectrum of butanethiol in Fig 3.3a shows three well-resolved bands which belong to the methyl terminal group (see Table 3.1). The C-H stretching modes of the methylene groups did not appear. This result is similar to previous spectra of butanethiols chemisorbed on gold film[3-8,3-9]. However, it differs from a recent report of the vibrational spectrum of hexanethiol on a Au(111) single crystal[3-10] which shows five broad C-H stretching bands and intense methylene modes. The spectrum of dibutylsulfides (shown in Fig 3.3b) chemisorbed on Au(111) consists of three broad bands. Unlike the butanethiol, the methylene bands were observed (see Table 3.1) at 2924 and 2853 cm^{-1}. The widths and wavenumbers of the C-H stretching modes of the methylenes indicate that the dibutylsulfides form a disordered monolayer[3-8]. The vibrational spectrum of dibutylsulfides adsorbed on a gold film evaporated on mica consists of three overlapping methyl C-H stretching modes[3-2]. The cyclic voltammogram of butanethiol (shown in Fig 3.4a) shows a sharp reductive peak, which is at -0.85 V, and when the potential is swept back (to positive potential), we find a small oxidative readsorption peak. In the cyclic voltammogram of dibutylsulfide shown in Fig 3.4b, there is a broad reductive peak at -0.92 V. We think that this is due to the disorder of the monolayer formed by dibutylsulfide as

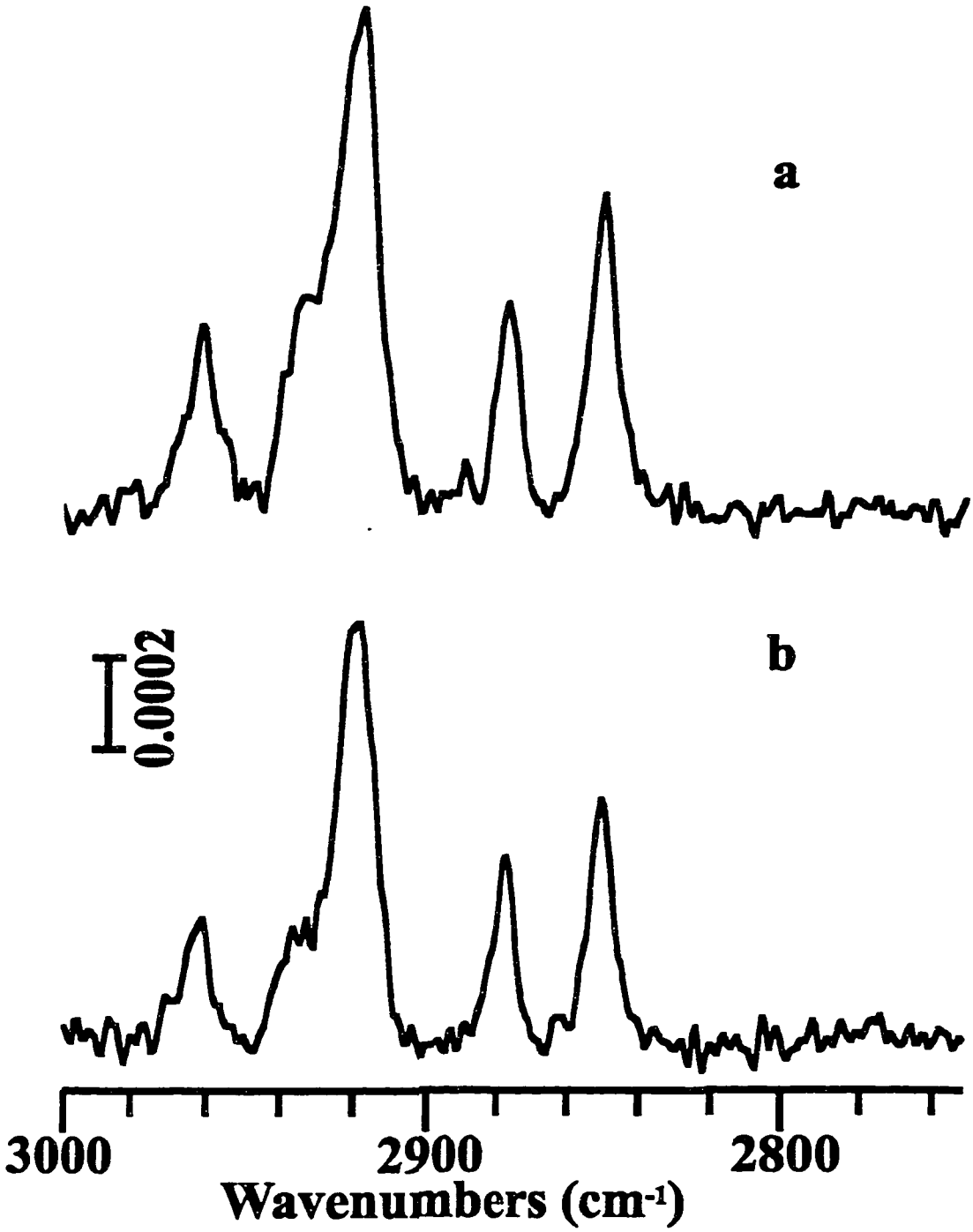

Fig 3.2 Infrared absorbance spectra of a monolayer of (a) hexadecanethiol, (b) hexadecyldisulfide chemisorbed on Au(111).

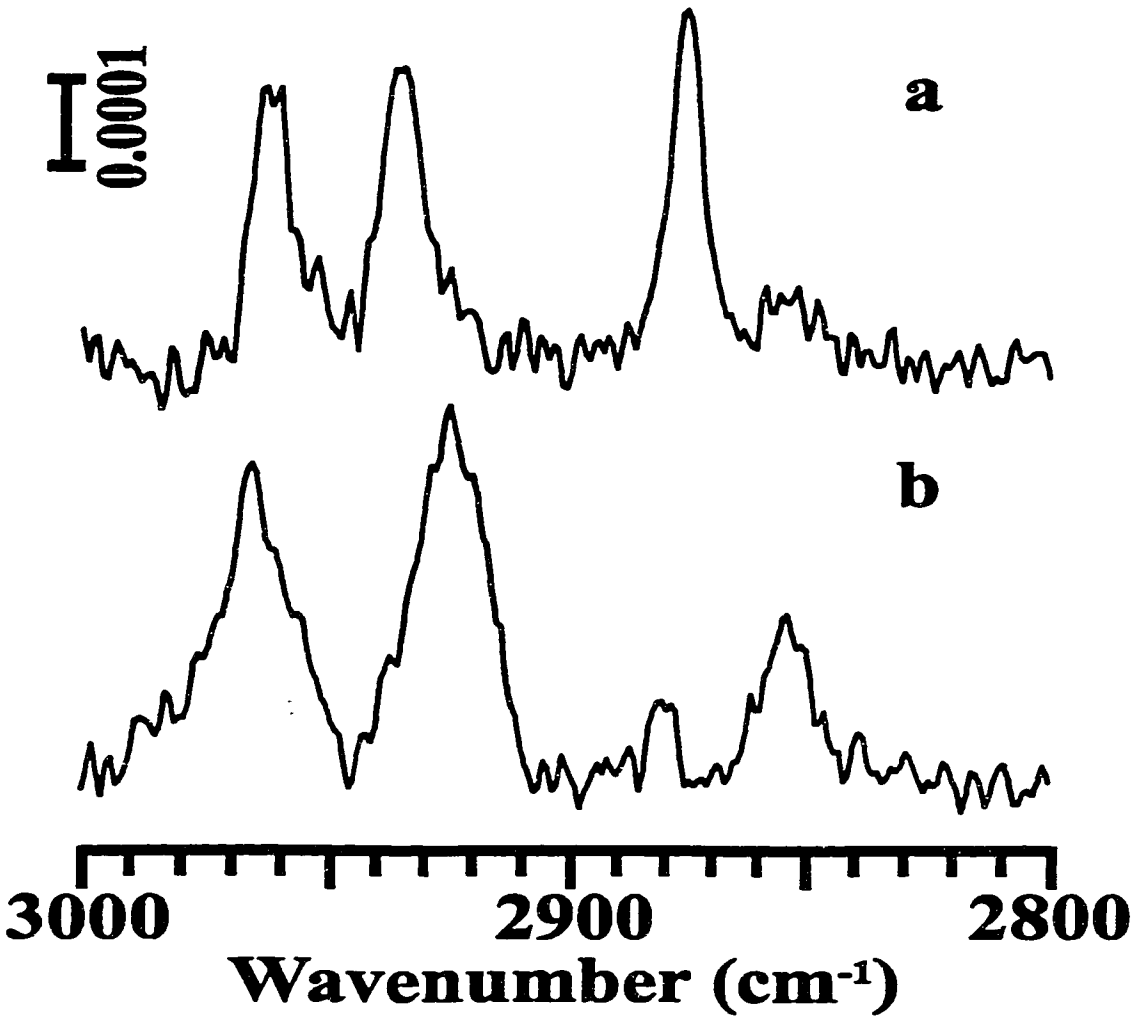

Fig 3.3 Infrared absorbance spectra of a monolayer of (a) butanethiol, (b) dibutylsulfide chemisorbed on Au(111).

	$-CH_3(\nu_a,ip)$	$-CH_3(\nu_s)$	$-CH_2(\nu_a)$	$-CH_3(\nu_s)$	$-CH_2(\nu_s)$
C_4H_9SH	2964	2935	-----	2875	-----
$(C_4H_9)_2S$	2966	-----	2924	-----	2853
$C_8H_{17}SH$	2963	2934	2922	2877	2850
$(C_8H_{17})_2S$	2965	2936	2922	2877	2850
$C_{12}H_{25}SH$	2964	2936	2919	2878	2850
$(C_{12}H_{25})_2S$	2964	2936	2922	2877	2850
$C_{16}H_{33}SH$	2963	2935	2919	2877	2850
$(C_{16}H_{33})_2S_2$	2962	2935	2919	2878	2850

Table 3.1 Assignments and wavenumbers of the C-H stretching bands of the vibrational absorbance spectra in Fig 3.2, Fig 3.3, Fig 3.5 and Fig 3.6. $-CH_3(\nu_a,ip)$ is the asymmetric in-plane C-H stretching mode of the CH_3 group, $-CH_3(\nu_s)$ are the symmetric C-H stretching modes of the CH_3 group, split by a Fermi resonance interaction with a CH_3 bending mode. $-CH_2(\nu_a)$ and $-CH_2(\nu_s)$ are the asymmetric and symmetric C-H stretching modes respectively.

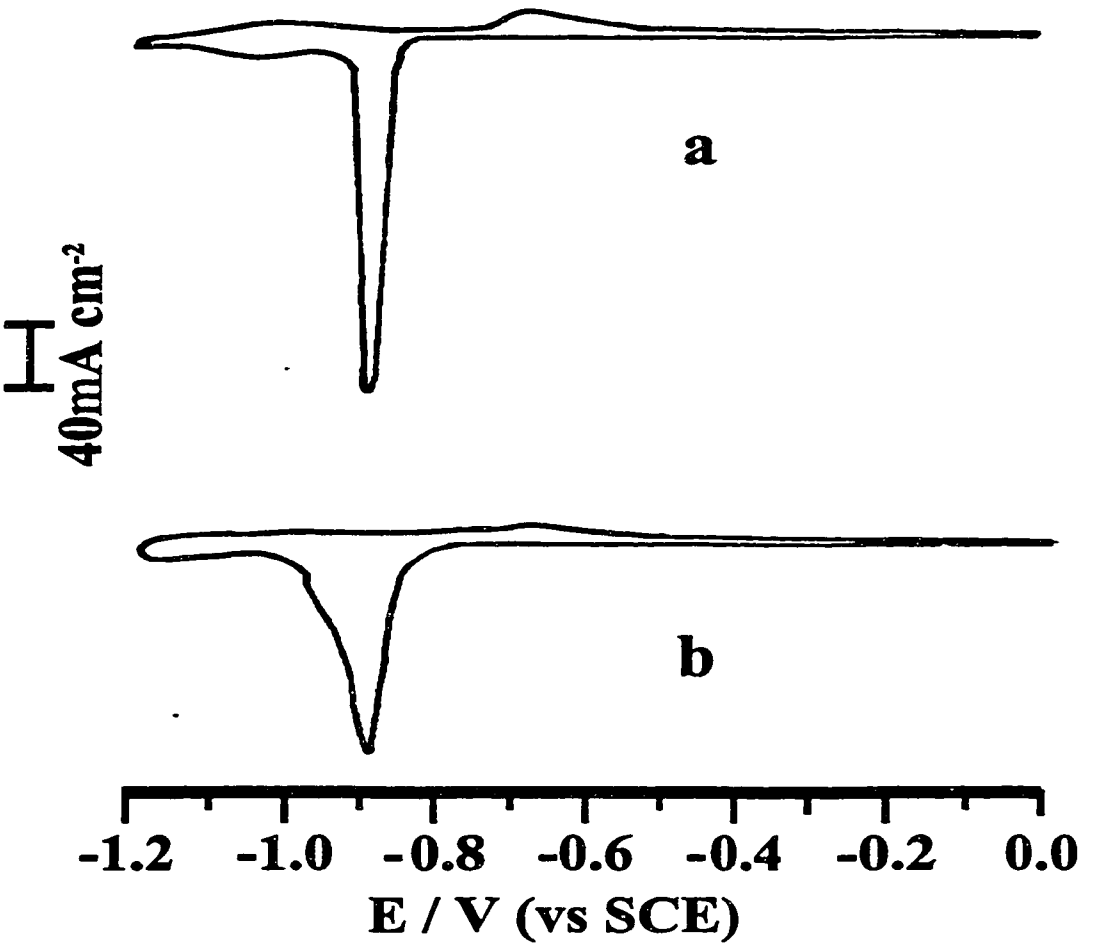

Fig 3.4 Cyclic voltammograms of (a) butanethiol, (b) dibutylsulfide chemisorbed on Au(111) in 0.1 M KOH with a scan rate of 100 mV s^{-1}.

shown by the vibrational spectrum, which leads to a better blocking of the surface.

In the case of the thiols and the sulfides with longer alkane chains (8 and 12 carbons were used), the vibrational spectra are very similar. The spectra of the monolayer formed by octanethiol (Fig 3.5a) and dioctylsulfide (Fig 3.5b) show five C-H stretching bands. The bands at 2963, 2934 and 2877 cm^{-1}, are assigned to the terminal methyl group. The other two bands, located at 2922 and 2850 cm^{-1} are related to the methylene group (see Table 3.1). The wavenumbers of the methylene's C-H stretching bands are indicative of a relatively ordered monolayer[3-11]. The slightly different intensities of the C-H stretching modes in these two spectra indicate that the orientations of the aliphatic chains of octanethiols and dioctylsulfides are very similar.

The vibrational spectra of the dodecanethiol (Fig 3.6a) and didodecylsulfide (Fig 3.6b) consist of five C-H stretching bands. The wavenumbers and the intensities of those bands (see table 3.1) in the two spectra are almost identical (within the experimental uncertainties). The wavenumbers of the C-H stretching modes for both monolayers are typical of alkanes in a crystalline state[3-11]. The spectrum of dodecanethiol is similar to a previous report[3-8], but this is not the case for the didodecylsulfide. Our spectra of the didodecylsulfide chemisorbed on a Au(111) single crystal differs from the previous reports[3-1,3-3] of the didodecylsulfide chemisorbed on a gold film. One study revealed spectra consisting of two broad C-H methylene bands at 2925 and 2853 cm^{-1}. Another study showed two broad methylene bands at 2926 and 2855 cm^{-1} with weak, unresolved, methyl bands. The wavenumbers and widths of the methylene bands in these studies are indicative of liquid-like monolayers. The cyclic voltammograms of these long chain thiols and sulfides shown in Fig 3.7 and Fig 3.8 are also similar (see discussion below).

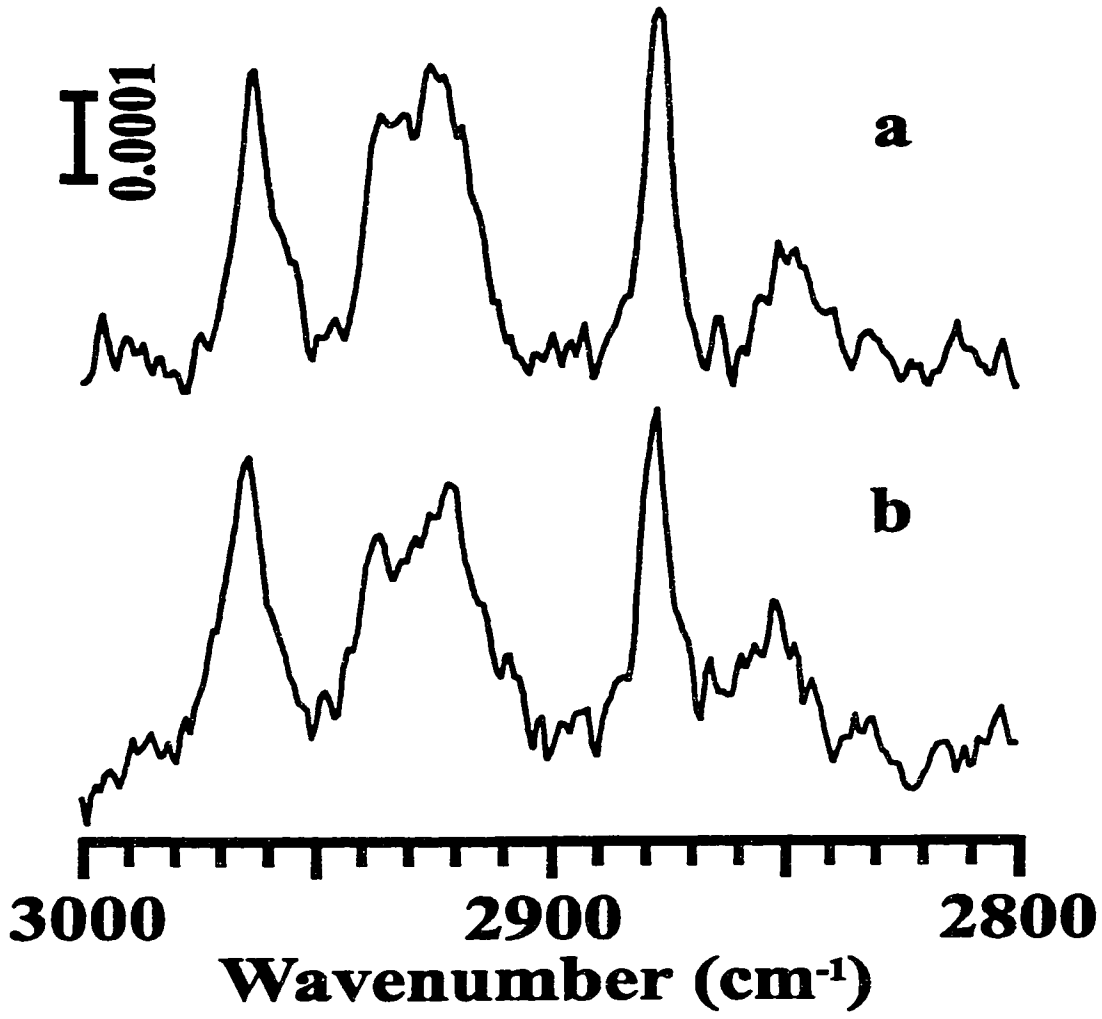

Fig 3.5 Infrared absorbance spectra of a monolayer of (a) octanethiol, (b) dioctylsulfide chemisorbed on Au(111).

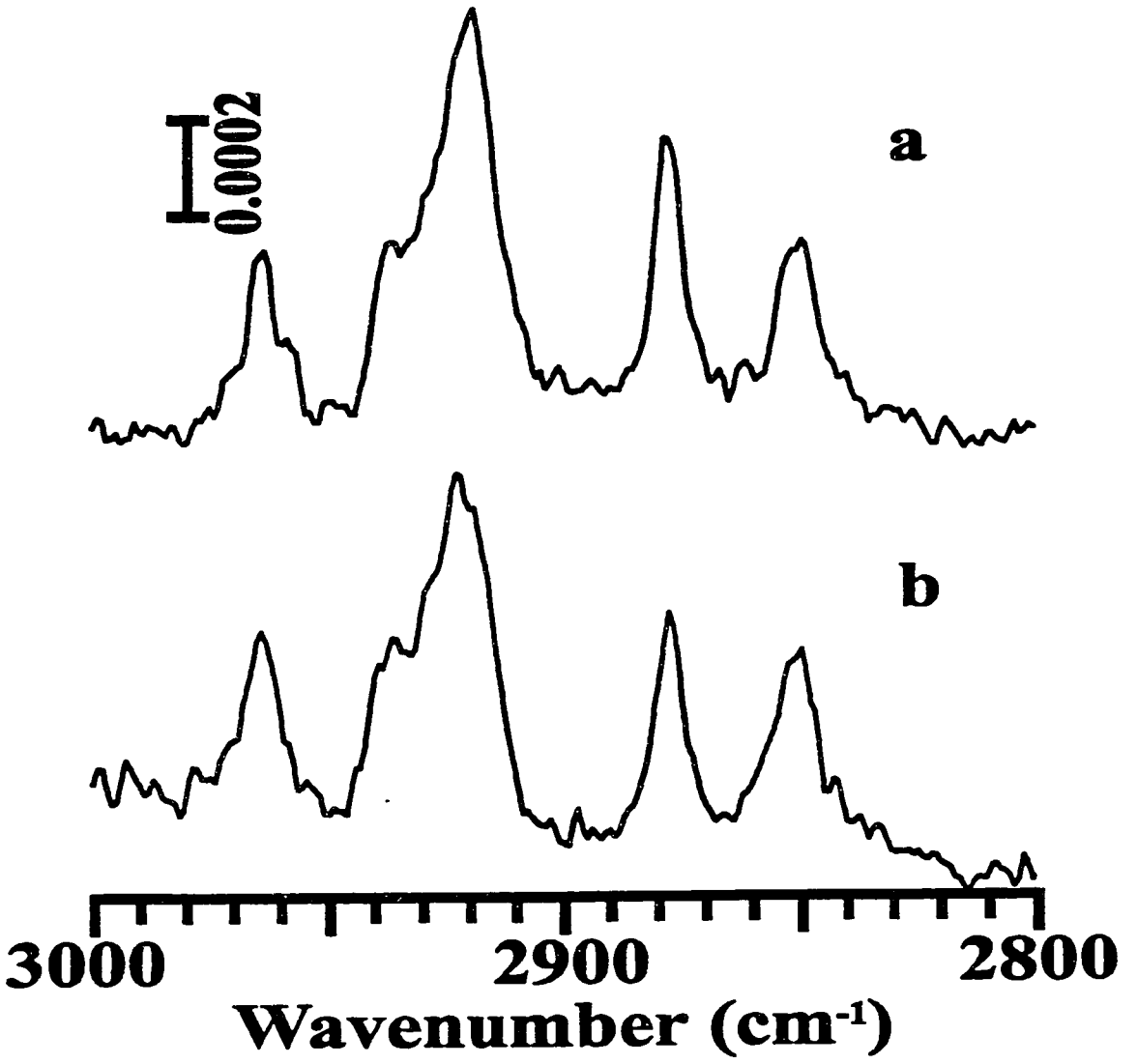

Fig 3.6 Infrared absorbance spectra of a monolayer of (a) dodecanethiol, (b) didodecylsulfide chemisorbed on Au(111).

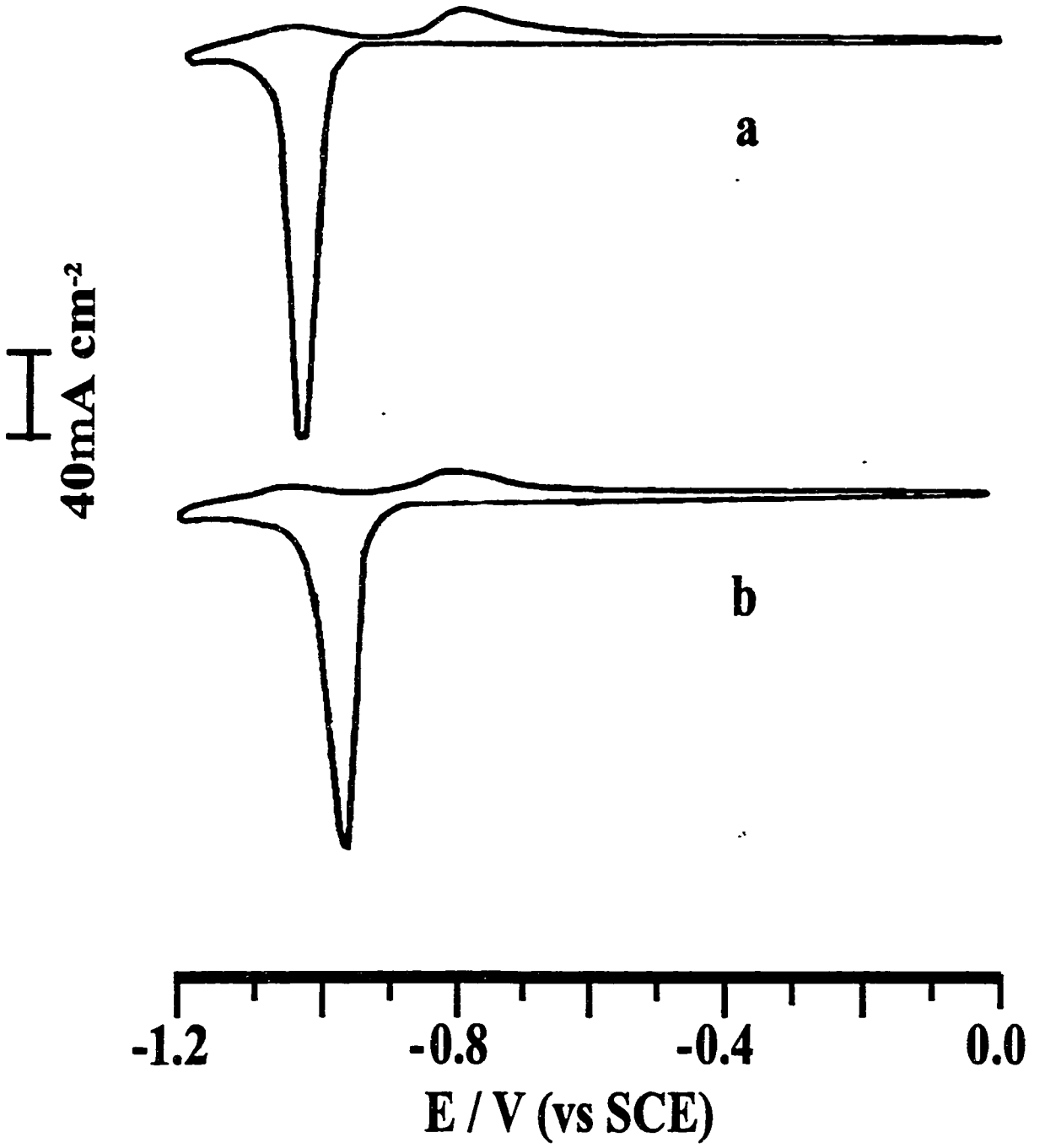

Fig 3.7 Cyclic voltammograms of (a) octanethiol, (b) dioctylsulfide, chemisorbed on Au(111) in 0.1 M KOH with a scan rate of 100 mV s^{-1}.

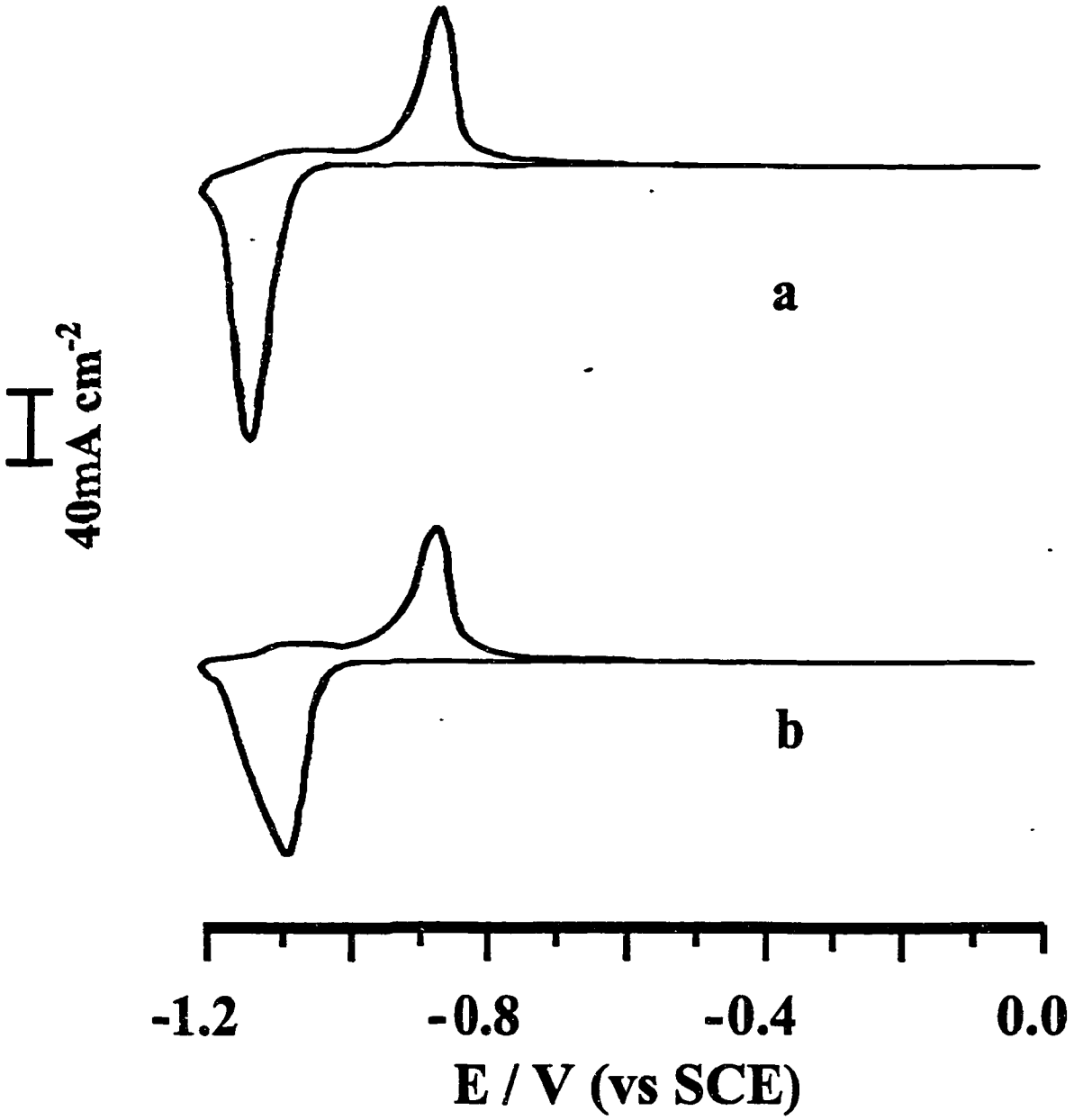

Fig 3.8 Cyclic voltammograms of (a) dodecanethiol, (b) didodecylsulfide, chemisorbed on Au(111) in 0.1 M KOH with a scan rate of 100 mV s^{-1}.

The potential of the maximum reductive current, E_p (shown in Table 3.2), in the cyclic voltammograms of the reduction of thiols becomes more negative as the number of carbons in the alkane chain increases. This agrees with a previous report[3-12]. The symmetric dialkylsulfides follow the same trend as the alkanethiols. The integrated charges of reductive current peaks (shown in Table 3.2) for all the compounds range from 95 $\mu C\ cm^{-2}$ to 105 $\mu C\ cm^{-2}$. The monolayer formed by the dibutylsulfides is reduced at more negative potential (-0.92 V) than the butanethiols (-0.85 V). For the other two longer chain sulfides, the reverse order is observed. The alkanethiols are reduced at more negative potential (-1.08 V for the octanethiol and -1.20 V for the dodecanethiol) than the dialkylsulfides (-1.01 V for the dioctylsulfide and -1.13 V for the didodecylsulfide). We also notice that reductive current peaks of the sulfides are larger than those of the thiols. Our voltammetric results agree with previous voltammograms of the reduction of butanethiols and dibutylsulfides chemisorbed on gold films[3-2].

We also observed the increase of the oxidative redeposition following the reductive desorption of the longer chain thiols and sulfides. The cyclic voltammograms of the dodecanethiol and didodecylsulfide monolayers in 0.1 M KOH (shown in Fig 3.8) show the oxidative current peaks at the same potential (-0.92 V) and their integrated charges are equal to 70% of the reductive charge (70 $\mu C\ cm^{-2}$). The integrated oxidative charges of the monolayer formed by octanethiols and dioctylsulfides in the 0.1 M KOH (shown in Fig 3.7) are only 18 $\mu C\ cm^{-2}$. But when those monolayers are put in a 0.1 M $KClO_4$ solution, their cyclic voltammograms are identical (shown in Fig 3.9) and display two oxidative peaks at -0.73 V and -0.56 V which integrate to 55 $\mu C\ cm^{-2}$. Hence a larger fraction of the reduced molecules are oxidatively redeposited in a solution of a lower pH. In the case of the alkanethiols, the increase of the oxidative redeposition of the reduced thiols in the neutral solution could be explained by the protonation of the thiolates (the product of the reduction) to form a thiol. The thiol has a lower solubility than a thiolate and thus remains at the electrode surface and can thus be oxidatively

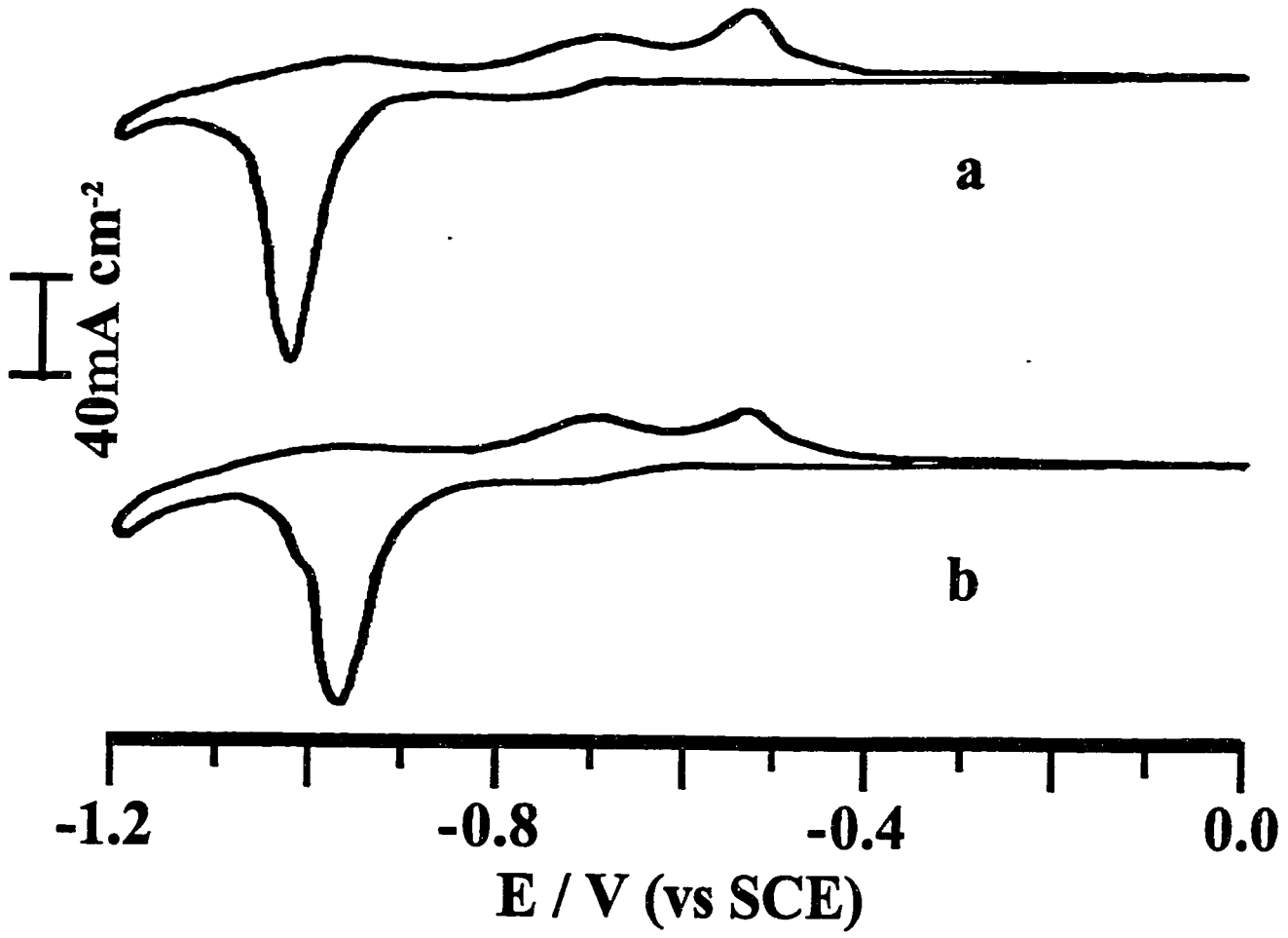

Fig 3.9 Cyclic voltammograms of (a) octanethiol, (b) dioctylsulfide, chemisorbed on Au(111) in 0.1 M $KClO_4$ with a scan rate of 100 mV s^{-1}.

redeposited[3-13]. Since the symmetric dialkylsulfides have oxidative currents identical to those of the alkanethiols at different pHs, their product of reduction must be the same, a thiolate.

	Q_{red} (μAcm^{-2}) (±8%)	Q_{ox}(μAcm^{-2}) (±10%)	E_p/V(vs. SCE) (±0.02V)
C_4H_9SH	95	<10%	-0.85
$(C_4H_9)_2S$	97	<10%	-0.92
$C_8H_{17}SH$	108	18	-1.08
$(C_8H_{17})_2S$	108	19	-1.01
$C_{12}H_{25}SH$	111	77	-1.20
$(C_{12}H_{25})_2S$	107	70	-1.13
$C_{16}H_{33}SH$	115	93	-1.18
$(C_{16}H_{33})_2S_2$	110	92	-1.19

Table 3.2 Reduction Peak potential, E_p, reductive charge, Q_{red}, oxidative charge, Q_{ox}, in cyclic voltammograms shown in Fig 3.1 , Fig 3.4, Fig 3.7 and Fig 3.8.

To further verify that the dialkylsulfides form a thiolate monolayer and that their reductive desorption is a one-electron process, we did chronoamperometric measurements. If the reduction of the monolayer formed by the dialkylsulfides need more than one electron, the current transient should be slower than the one-electron process of an alkanethiol[3-14]. The chronoamperograms of the reduction of monolayer formed by dibutylsulfides following a potential step from -0.3 V to different final potentials (shown in Fig 3.10) display smooth current transients. Their duration decreases from 0.1 s to 0.01 s when the final potential changes from -1.10 V to -1.25 V. Their shape and time duration are similar to those observed for butanethiols[3-14]. This indicates that the reduction follow a hole-nuclei mechanism[3-14] similarly to what was reported for the reductive desorption of a monolayer of butanethiols.

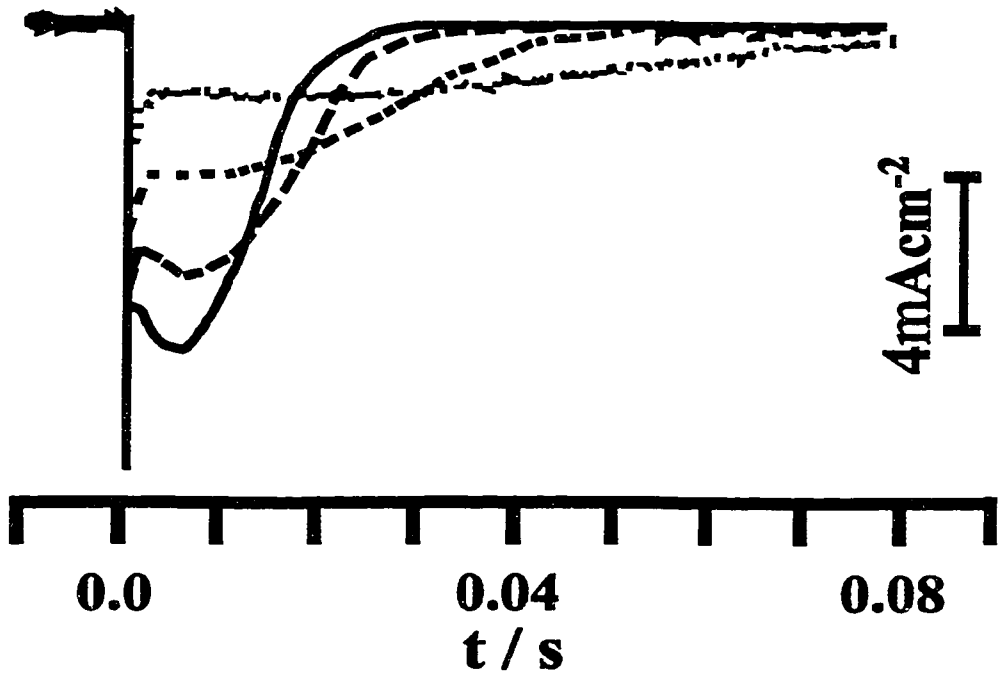

Fig 3.10 Chronoamperograms of dibutylsulfide in 0.1 M KOH for a potential step from -0.3 V to -1.10 V (dotted) ; -1.15 V (short dashed) ; -1.20 V (long dashed) ; -1.25 V (solid).

To estimate the adsorbate coverage(Γ) on the Au(111) electrode surface, the reductive charges in Table 3.2 will be used. However the total reductive charge is composed of a faradaic charge (ΔQ_F) and a capacitive charge (ΔQ_C). The coverage is calculated from the faradaic contribution only. Thus the capacitive charge must be subtracted from the total charge[3-15]. The following is a brief summary of the calculation of the capacitive charge (as shown in Fig 3.11). The capacitive charge ΔQ results from the difference between the double layer charge of the coated electrode Q_1 and the uncoated electrode Q_2. The uncoated electrode is not a perfect capacitor[3-16] and Q_2 is obtained from chronocoulometric measurements[3-17], which is -32 $\mu C\ cm^{-2}$ at -1.1 V. The coated electrode is assumed to be a perfect capacitor, so $Q_1 = C(E_1-E_{1,pzc})$, where C is the electrode capacitance at E_1 and $E_{1,pzc}$ is the potential of zero charge (PZC) of coated single crystal electrode. We assume $E_{1,pzc}$ is located between -0.45 V, which is the maximum of the eletrocapillary curve of a thiol-coated polycrystal electrode[3-18], and 0.28 V, the PZC of the uncoated Au(111) electrode. The sulfur coverage of dialkylsulfide monolayer was estimated from the reductive charge assuming that the reduction requires one-electron per adsorbate. So $\Gamma = Q/F$, where Q is the faradaic charge and F is the Faraday constant. The faradaic charge is between 66 and 76 $\mu C\ cm^{-2}$. This gives coverages ranging from 7 to 8×10^{-10} mol cm^{-2} (shown in Table 3.4). These sulfur coverages are the same (within the experimental uncertainties) as those measured previously for alkanethiols[3-12,3-13,3-15], which are around 7.6×10^{-10} mol cm^{-2}. The estimated coverages are consistent with the dissociative adsorption of the dialkylsulfides and the formation of one monolayer of thiolates.

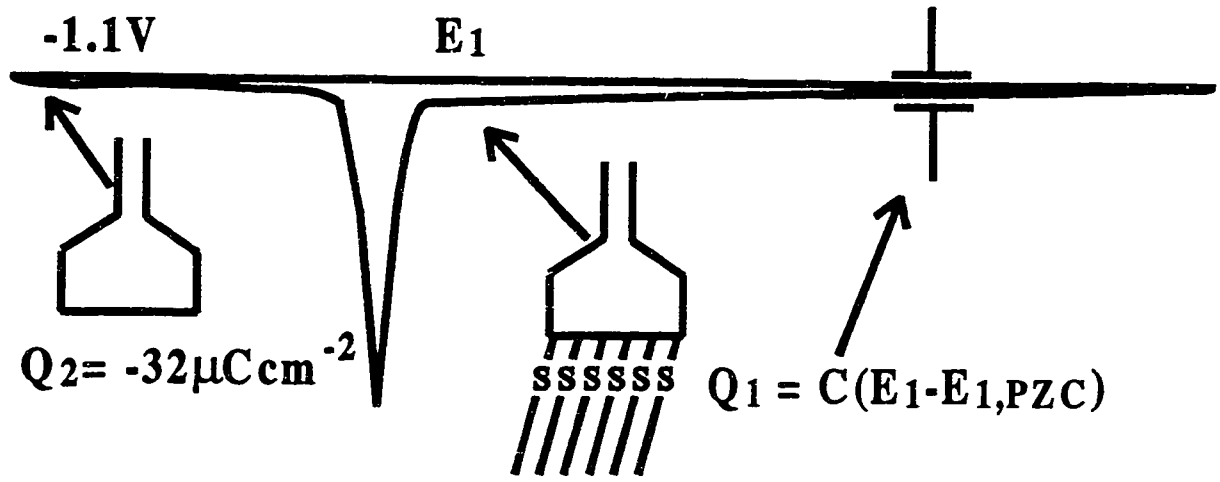

$$\text{Capacitive charge} = Q_2 - Q_1$$

Fig 3.11 Capacitive charge calculation

	$Q_C(\mu C\ cm^{-2})$ (±8%)	$Q_F(\mu C\ cm^{-2})$ (±8%)	$\Gamma(10^{-10}\ mol\ cm^{-2})$ (±8%)
C_4H_9SH	30	65	6.8
	27	68	7.1
$(C_4H_9)_2S$	31	66	6.9
	29	68	7.1
$C_8H_{17}SH$	31	77	8.0
	29	79	8.2
$(C_8H_{17})_2S$	31	78	8.1
	29	79	8.2
$C_{12}H_{25}SH$	31	80	8.3
	30	81	8.4
$(C_{12}H_{25})_2S$	31	76	7.8
	30	77	8.0

Table 3.3 Faradaic and capacitive charge contribution to the total reductive charge and the surface coverage of alkanethiols and dialkylsulfides on the Au(111) (see text for details).

3.2. Pentamethylene sulfide

From the comparison of the monolayers formed by dialkylsulfides and by alkanethiols, we know that the long chain dialkylsulfides dissociate and form an ordered monolayer of thiolates on a Au(111) single crystal. Therefore the alkane chain produced by the cleavage of one of the C-S bonds must leave the surface without disturbing the formation of an ordered monolayer of thiolates. The dissociation of the C-S bond upon adsorption of the sulfide yields reactive species. The homolitic cleavage of the C-S bond produces a radical and its heterolitic cleavage of the C-S bond produces a carbocation. Either of these products can react with other chemisorbed sulfides and disrupt the formation of an ordered monolayer. But our results show this is not happening for the dialkylsulfides. However our and previous results do not allow for the determination of the adsorption mechanism because one of the alkane chains leaves the surface and can not be detected. Pentamethylene sulfide, a cyclic sulfide, was chosen to study the C-S bond dissociation upon adsorption on a gold single crystal. In the case of pentamethylene sulfide once one of its C-S bonds is broken, the product will remain at the surface. This allows for the identification of the product of the dissociation of the sulfide.

The vibrational spectrum of the monolayer formed by the pentamethylene sulfide after incubation of the Au(111) in a 0.01 M ethanolic solution of this compound is shown in Fig 3.12. This spectrum shows that an aldehyde has been formed[3-19]. There are four bands in this spectrum. The presence of an aldehyde was proved by the CO stretching mode at 1730 cm^{-1} and two C-H stretching modes at 2820 cm^{-1} and 2725 cm^{-1} (assigned to a Fermi resonance of the C-H stretching mode of the aldehyde C-H band with the overtone of its C-H bending mode). The other broad C-H stretching band at 2929 cm^{-1} is assigned to the methylene groups.

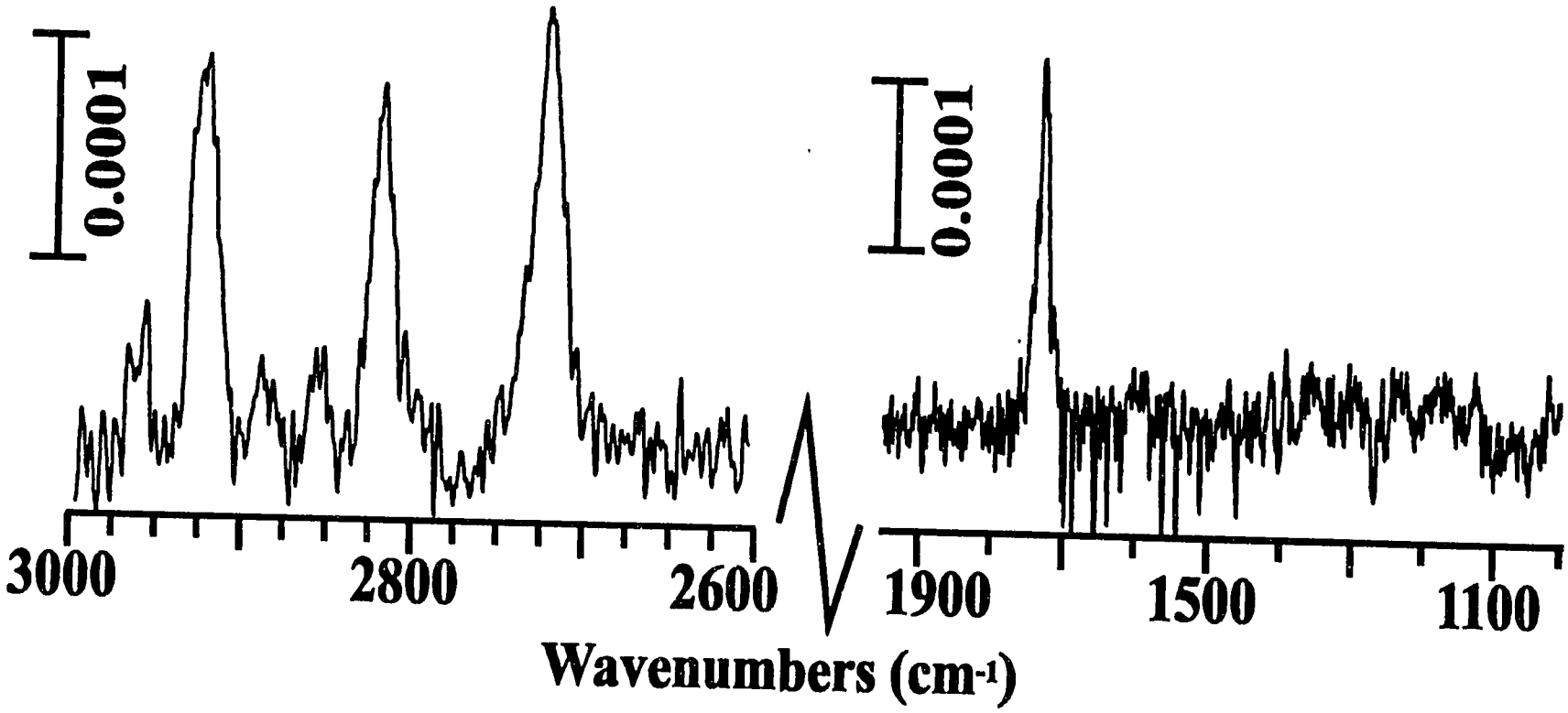

Fig 3.12 Infrared absorbance spectrum of a monolayer formed by incubating a Au(111) in a 0.01M pentamethylene sulfide ethanolic solution for one hour. Four bands are observed, they are: $-CH_2$,ν_a (2929 cm^{-1}); the Fermi resonances of the C-H stretching mode for aldehyde (2820 cm^{-1} and 2725 cm^{-1}) ; the -C=O stretching mode of an aldehyde (1730 cm^{-1}).

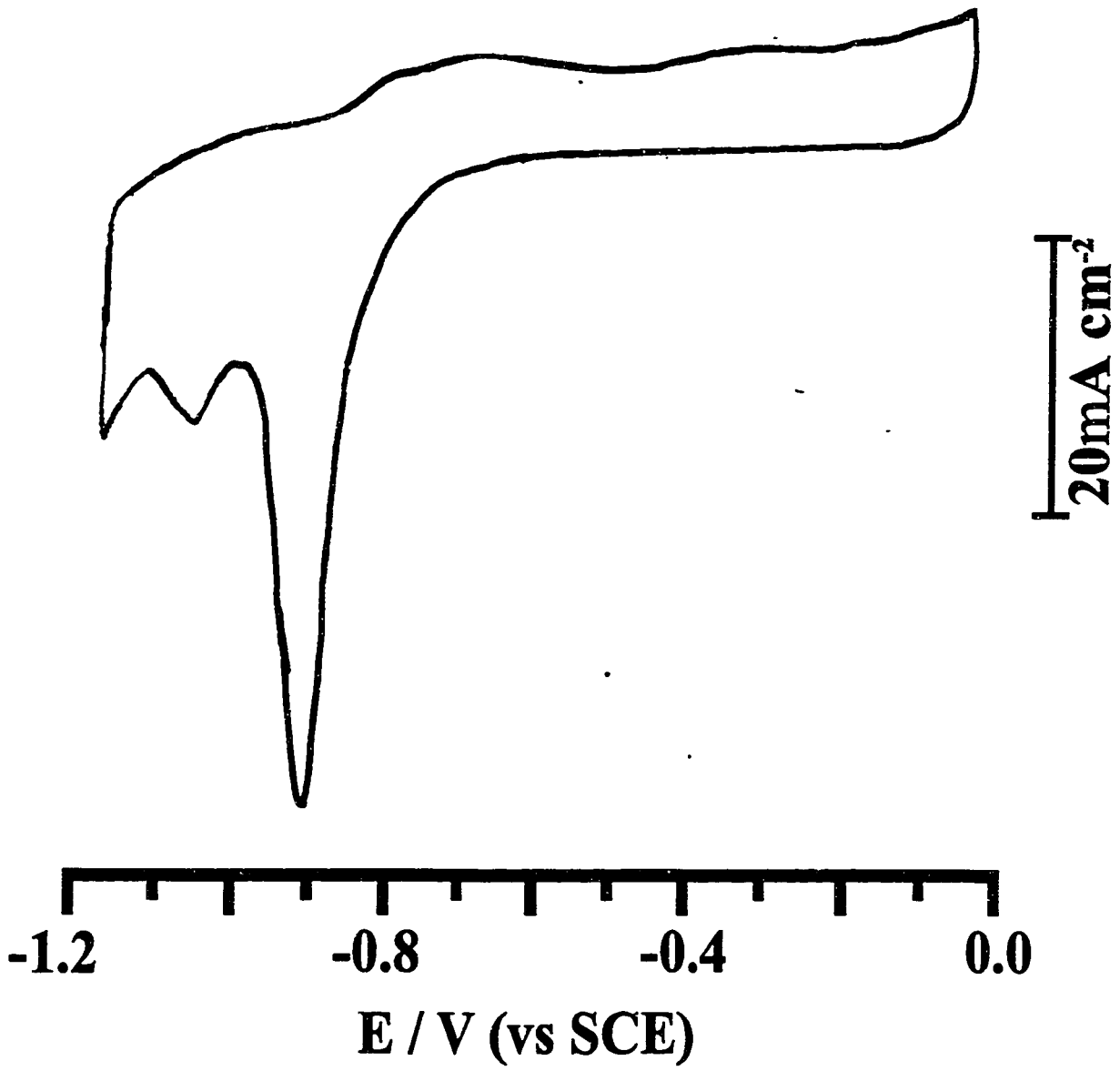

Fig 3.13 Cyclic voltammogram of pentamethylene sulfide chemisorbed on Au(111) in 0.1 M KOH at a scan rate of 100 mV s^{-1}.

The cyclic voltammogram of pentamethylene sulfide in Fig 3.13 reveals one broad reduction peak at -0.94 V which integrates to 100 μC cm^{-2}. The voltammogram of pentanethiol under the same conditions shows one peak at -0.97 V which integrates to 105 μC $cm.^{-2}$. The reductive charges and E_ps suggest that all the pentamethylene sulfide is dissociated and adsorbed as aldehyde-terminated thiolates.

The formation of an aldehyde indicates that the chemisorbed cyclic sulfide is oxidatively dissociated. No aldehyde-terminated thiols are detected in the GC-MS analysis of the incubation solution thus the oxidation of the pentamethylene sulfide must occur at the surface. Since more than one species (traces of water and molecular oxygen) in our system can provide oxygen to form the aldehyde, we did the following experiments. First, we added water into the incubation solution to form a 0.01 M pentamethylene sulfide, 1% water/ethanol solution. The Au(111) single crystal was then incubated in it. A vibrational spectrum identical to the one described in the previous paragraph was observed. Thus the water does not play a role in the oxidation of the pentamethylene sulfide.

Then, we formed a monolayer of the pentamethylene sulfide by incubating in a argon-degassed ethanolic solution. The vibrational spectrum of this monolayer in Fig 3.14 shows the C-H bands (2834 cm^{-1} and 2720 cm^{-1}) of the aldehyde but their intensities have decreased. A broad band due to the asymmetric methylene stretching at 2925 cm^{-1} dominates the spectrum of the C-H stretching bands. The increased intensity of the methylene mode indicates that the chain is more parallel to the surface compared to the spectrum in Fig 3.12. This observation agrees with the lower coverage shown by the cyclic voltammogram (shown in Fig 3.15) which shows one reductive peak at -0.94 V where integrated charge is only 85 μC cm^{-2}. Another experiment confirms the oxidation of pentamethylene sulfide by oxygen. First, the incubation solution was degassed by the oxygen for about one hour, followed by the incubation of the gold substrate. The vibrational spectrum of the resulting monolayer

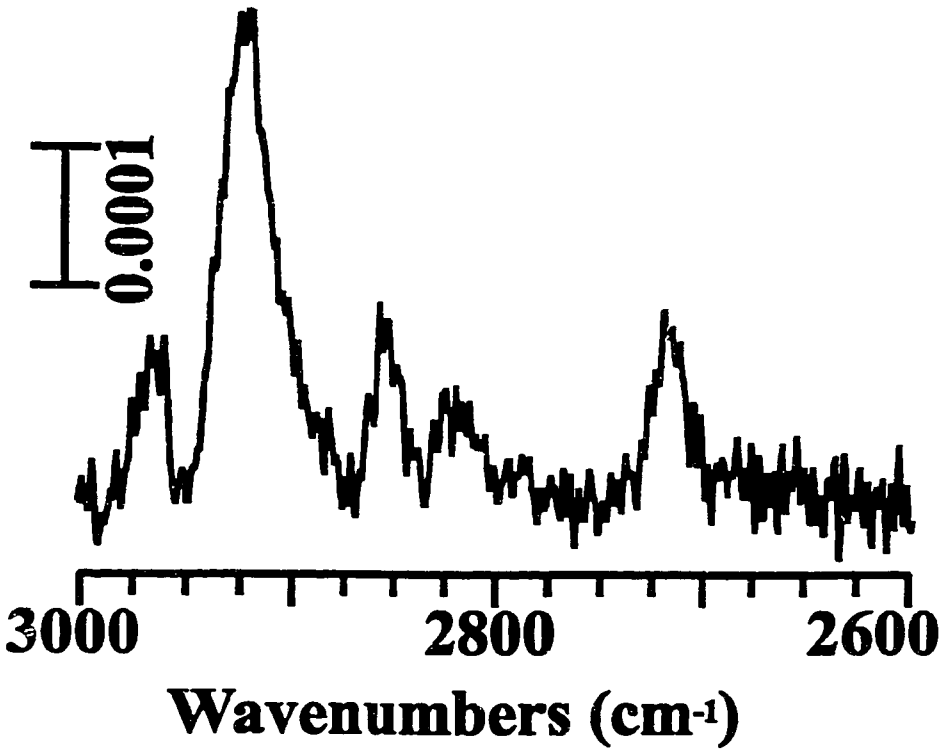

Fig 3.14 Infrared absorbance spectrum of a monolayer formed by incubating a Au(111) substrate in 0.01 M pentamethylene sulfide ethanolic solution argon-degassed for one hour.

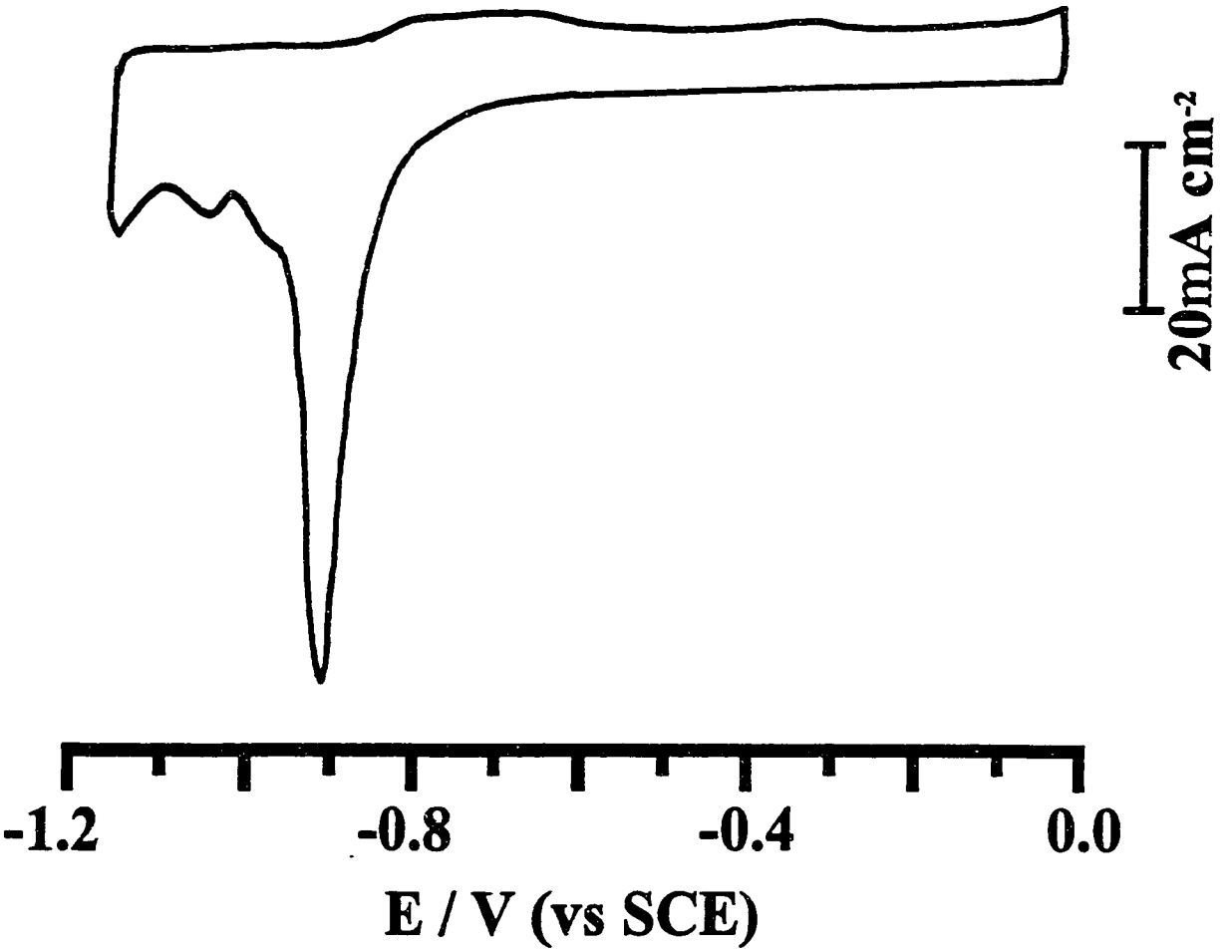

Fig 3.15 Cyclic voltammogram of the monolayer formed by incubating Au(111) in a 0.01 M argon-degassed pentamethylene sulfide solution (0.1 M KOH) with scan rate 100 mV s^{-1}.

was identical to the one shown in Fig 3.12. These experiments proved that the formation of the aldehyde is due to oxidation of the sulfides by molecular oxygen.

3.3. S_N2 reactions on Au(111) surface

The oxidative dissociation of the cyclic sulfide is not occurring in solution so there should be a precursor to the oxidative dissociation. We suggest that the first step in the dissociation process is the formation of a reactive chemisorbed pentamethylene sulfide on the Au(111) surface. We use S_N2 chemistry to verify this suggestion. A nucleophilic substitution should be possible because the C-S bond in the sulfide would be weakened and the sulfur should be electron deficient.

Different nucleophiles (ammonia, acetate, hydroxyl and ethanolate) of various strengths, but all weaker than the thiolate, were used. Those nucleophiles were directly added into the incubation solution. In the GC-MS analysis there are only pentamethylene sulfide and the nucleophiles in the solvent. We can thus rule out that nucleopilic reactions are occurring in the incubation solution.

The Au(111) single crystal was immersed in the incubation solution which contain different nucleopiles for one hour and the vibrational spectra of the resulting monolayers are shown in Fig 3.16 to Fig 3.19. In all those spectra we observed, in addition to the new bands which belong to the different product of the nucleopilic attack, a C=O stretching band of an aldehyde at 1730 cm^{-1}. This indicates that the oxidation of pentamethylene sulfide is still occurring.

The weakest nucleophile, ammonia, reacts with the pentamethylene sulfide on the Au(111) surface and forms a primary amine. This was proved by the C-N stretching mode at 1120 cm^{-1} observed in Fig 3.16. The NH_2 stretching and bending modes were not observed but these modes are expected to be weak[3-19]. A C-H stretching band of the methylene group is observed at 2928 cm^{-1}. The aldehyde C-H

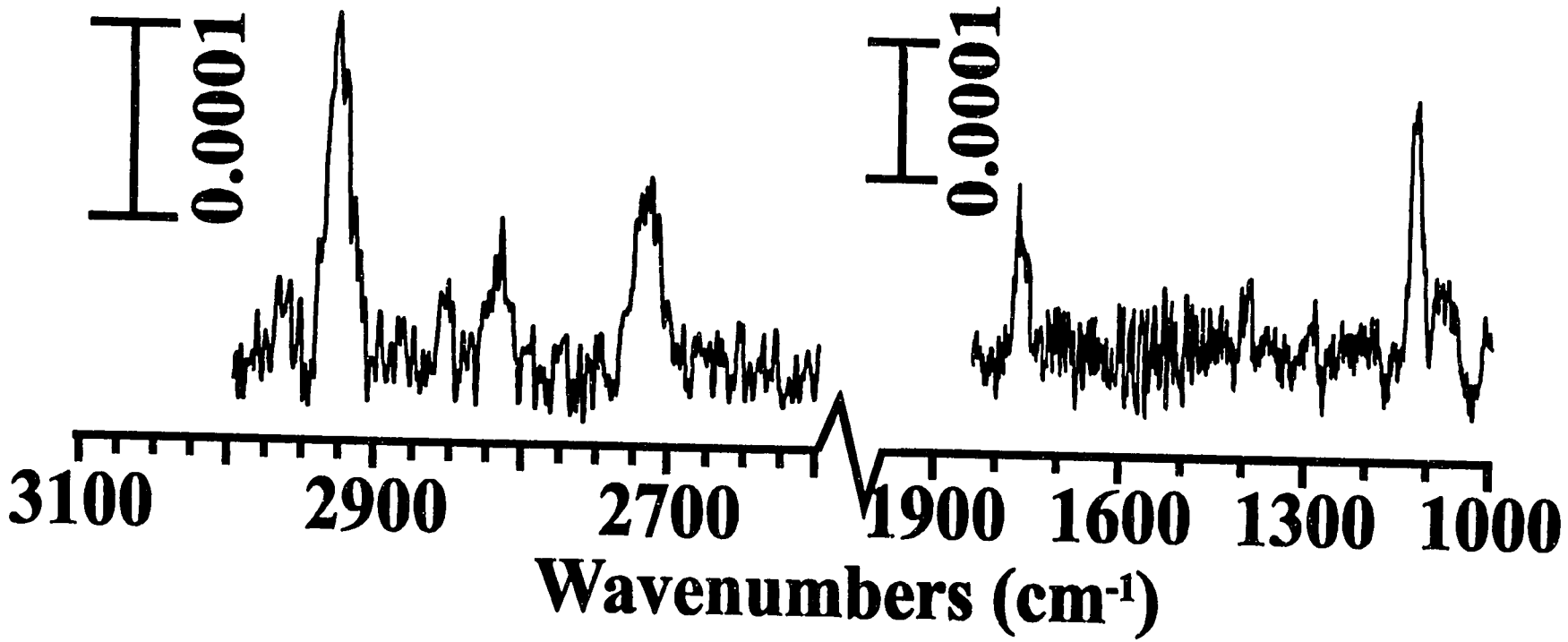

Fig 3.16 Infrared absorbance spectrum of a monolayer formed after a one hour incubation of a Au(111) in a solution which contains 0.01 M pentamethylene sulfide and 0.01 M ammonia in ethanol. Five bands are observed, they are $-CH_2, \nu_a$ (2929 cm^{-1}); Fermi resonance of C-H stretching mode of an aldehyde (2820 and 2725 cm^{-1}); the -C=O stretching mode of an aldehyde (1730 cm^{-1}) ; the C-N stretching mode primary amine (1120 cm^{-1}).

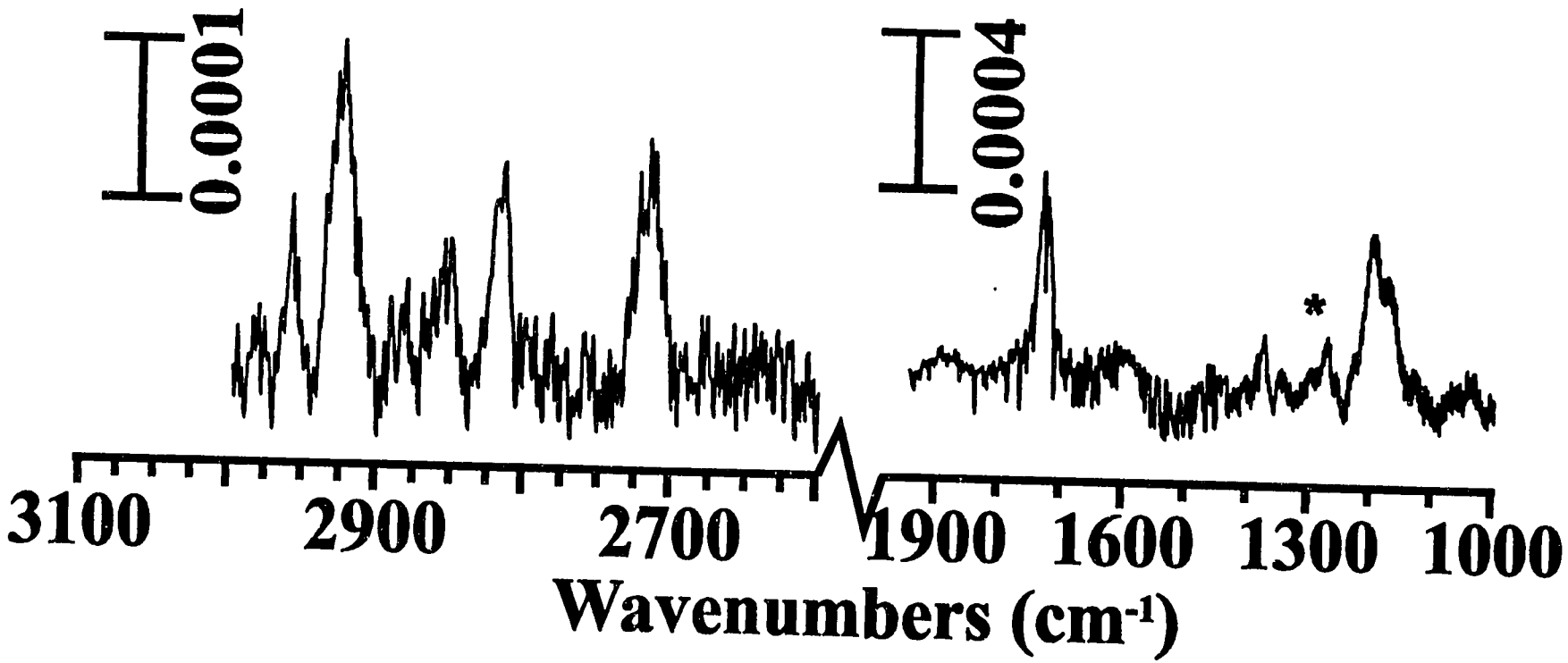

Fig 3.17 Infrared absorbance spectrum of a monolayer formed after a one hour incubation of a Au(111) in a solution which contains 0.01 M pentamethylene sulfide and 0.01 M sodium acetate in ethanol. Six bands are observed, they are $-CH_3$, ν_a (2960 cm^{-1}) ; $-CH_2$,ν_a 2929 cm^{-1} (2929 cm^{-1}) ; the Fermi resonance of C-H stretching mode of an aldehyde (2820 and 2725 cm^{-1}); the -C=O stretching mode of an aldehyde (1730 cm^{-1}) ; the C-O stretching mode of a ester (1204 and 1176 cm^{-1}).

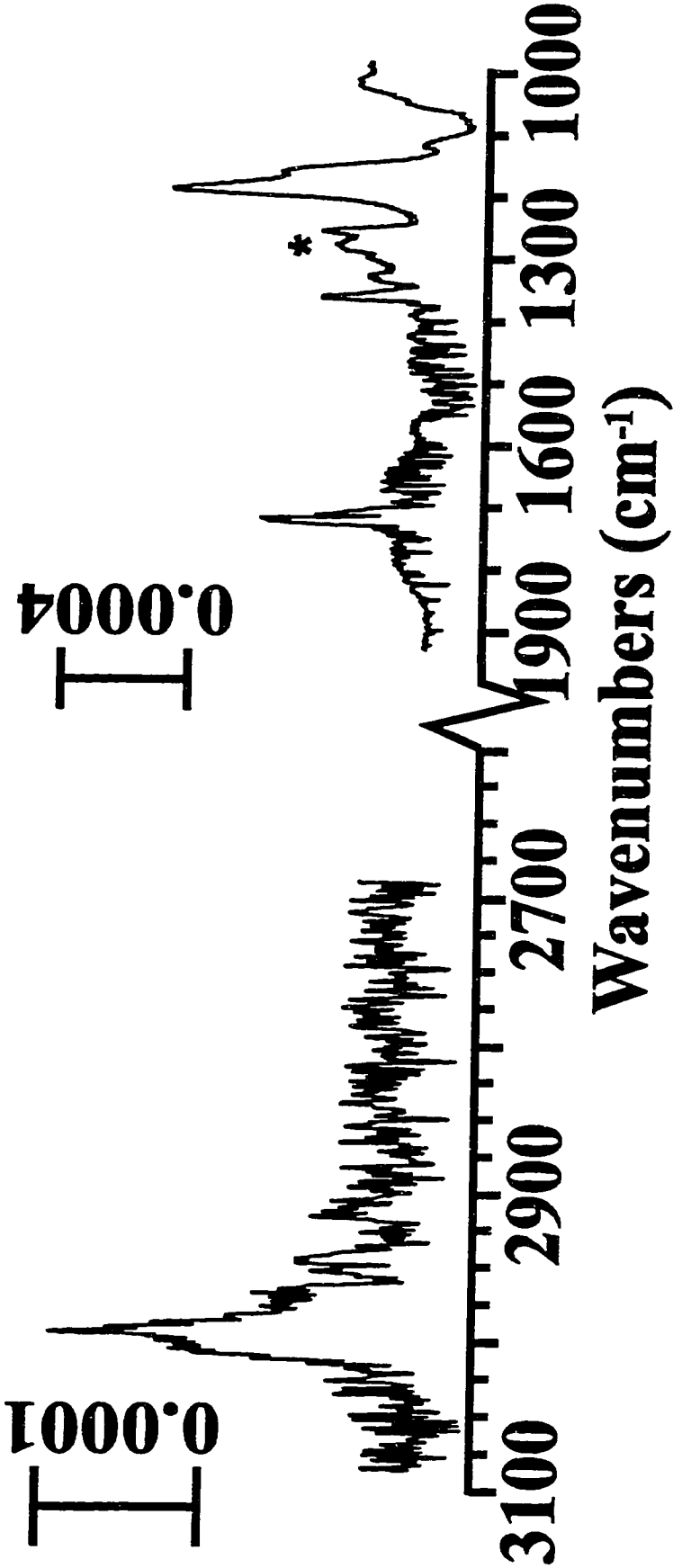

Fig 3.18 Infrared absorbance spectrum of a monolayer formed after a one hour incubation of a Au(111) in a solution which contains 0.01 M pentamethylene sulfide and 0.01 M KOH in ethanol. Four bands are observed, they are $-CH_2$ stretching mode (2984 cm^{-1}) ; -C=O stretching mode of an aldehyde (1730 cm^{-1}) ; C-O stretching mode of an ether (1206 and 1180 cm^{-1}).

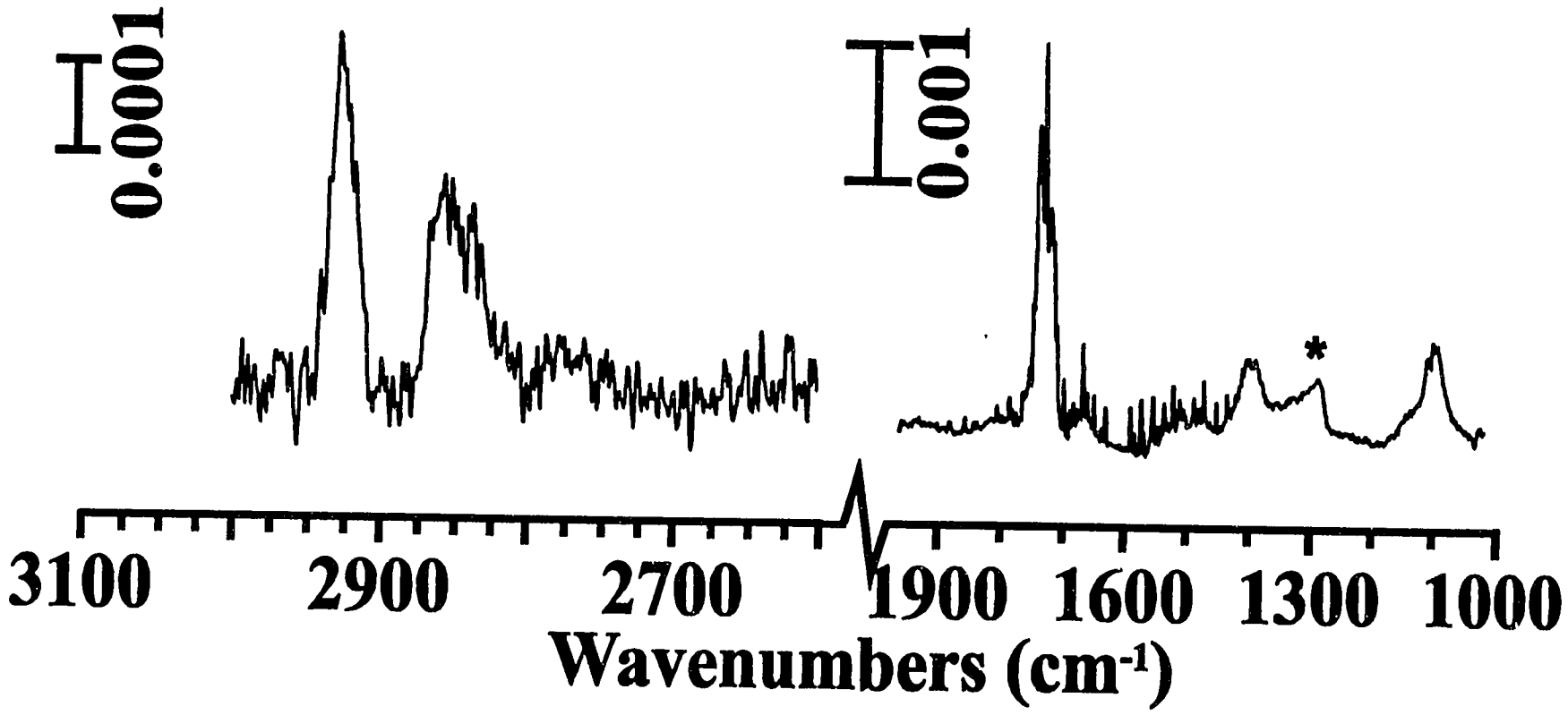

Fig 3.19 Infrared absorbance spectrum of a monolayer formed after a one hour incubation of a Au(111) in a solution which contains 0.01 M pentamethylene sulfide and 0.01 M KOH in 5% water/DMF. Four bands are observed, they are $-CH_2$ stretching mode (2926 and 2860 cm^{-1}) ; -C=O stretching mode of an aldehyde (1730 cm^{-1}) ; C-O stretching mode of a primary alcohol (1080 cm^{-1}).

stretching modes are visible and located at 2820 cm^{-1} and 2720 cm^{-1}. This result indicates that the chemisorbed sulfide is quite reactive since ammonia is a much weaker nucleopile than a thiolate.

A weak band at 1380 cm^{-1}, seen in Fig 3.17 to Fig 3.19, is tentatively assigned to the C-H bending mode of the aldehyde[3-11]. The peak indicated by * is due to the instrument(a strong and sharp absorption due to a coating on the optics).

Acetate reacts with the chemisorbed pentamethylene sulfide and forms an ester. This monolayer was obtained by incubating the Au(111) single crystal in a 0.01 M sodium acetate and 0.01 M pentamethylene sulfide ethanolic solution. The resulting vibrational spectrum is shown in Fig 3.17. In this spectrum, the two unresolved bands at 1204 cm^{-1} and 1176 cm^{-1} are assigned to the C-O stretching modes of an ester. The C=O stretching band of the ester is expected to be at about 1740 cm^{-1} and would overlap with the C=O stretching mode of the aldehyde. A band at 2960 cm^{-1} assigned to the methyl C-H stretching mode confirms the presence of an ester. A methylene C-H stretch is observed at 2927 cm^{-1} and the aldehyde C-H stretching modes are observed at 2820 cm^{-1} and 2718 cm^{-1}. Our results agree with the previous spectra of a methyl 16-mercaptohexadecanoate monolayer on gold[3-20] , which displayed a C=O mode at 1748 cm^{-1} and two C-O modes at 1207 cm^{-1} and 1179 cm^{-1}.

The vibrational spectrum recorded after an incubation of the Au(111) single crystal in a 0.01 M KOH, 0.01 M pentamethylene sulfide solution in ethanol is shown in Fig 3.18. In this spectrum, a C-O stretching mode is observed at 1206 cm^{-1} with a shoulder peak at 1180 cm^{-1}. There is another broad C-H stretching band at 2984 cm^{-1}. These bands are assigned to an ether[3-19]. The C-H stretching band of an ether was observed at 2982 cm^{-1} in a SFG (Sum Frequency Generation) spectra of those ethoxy-terminated thiols[3-21]. This result is unexpected since it requires the presence of ethanolates. In a 0.01 M KOH solution, the concentration of ethanolate is estimated

to be 10^{-4} M (based on a pK_a of 16 for the ethanol). Thus ethanolates must be stronger nucleophiles than the hydroxyls for the opening of the pentamethylene sulfide ring. The methylene C-H stretching modes are too weak to be observed. We believe that it is partially due to the repulsion between the ethers which causes disorder in the monolayer and decreases the intensity of these modes.

To use hydroxyl as a S_N2 reagent, we used DMF as a solvent because it does not react with KOH. An incubation solution containing 0.01 M KOH, 0.01 M pentamethylene sulfide solution in a 5% water/DMF solvent (5% water was added to help dissolve the KOH) was used. The vibrational spectrum of the monolayer obtained from this incubation solution in Fig 3.19 shows the typical vibrational bands of an alcohol. The band at 1080 cm^{-1} is assigned to a C-O stretch of a primary alcohol. The methylene stretching bands are visible at 2926 cm^{-1} and 2860 cm^{-1}. But we did not find the O-H stretching band. A C-O mode at 1070 cm^{-1} has been reported for a 16-mercaptohexadecanol adsorbed on gold[3-22]. The O-H stretching band was also absent in this study. These results give support to our assignment.

The identification of the products of the reaction of the pentamethylene sulfide and different nucleophiles by vibrational spectroscopy supports the presence of an activated chemisorbed sulfide.

The cyclic voltammograms of the reduction of the various monolayers of the nucleophile-terminated thiolates show that all the pentamethylene sulfides undergo either an S_N2 reaction or an oxidation. All the voltammograms of the monolayers of nucleophile-terminated thiolates display one reductive current peak. The potentials of the maximum reductive current, E_p (shown in Table 3.3), of the nucleophile-terminated pentanethiol vary. These are: -0.95 V for the amine-terminated, -0.89 V for the ester-terminated, -0.97 V for the ether-terminated and -0.84 V for the alcohol-terminated thiolate monolayer. All these E_p, except for the alcohol, are close to the potential of the maximum current of the aldehyde-terminated thiolate (-0.94 V)

and methyl-terminated thiolate (pentanethiol, -0.97 V). The values of the integrated charge of the reduction peak are: 95 $\mu C\ cm^{-2}$, for the amine-terminated thiol; 90 $\mu C\ cm^{-2}$, for the ester-terminated thiol; 105 $\mu C\ cm^{-2}$, for the ether-terminated thiol; and only 75 $\mu C\ cm^{-2}$, for the alcohol-terminated monolayers. The high values of the reductive charges, except for the alcohol, indicate a coverage close to that of a monolayer of the pentanethiols (105 $\mu C\ cm^{-2}$). We attribute the lower reductive charge of the alcohol-terminated thiolate to the use of DMF which is known to lead to a lower surface coverage[3-23].

Incubation solution	$Q_{red}(\mu Acm^{-2})$	E_p / V (vs. SCE)
0.1M Pentamethylene sulfide(PMS)	100	-0.94
0.1 M PMS, degas	85	-0.94
0.1 M PMS+ 0.1 M NH_3	95	-0.95
0.1 M PMS+ 0.1 M sodium acetate	90	-0.89
0.1 M PMS+ 0.1 M KOH	105	-0.97
0.1 M PMS + 0.1 M KOH in 5%H_2O / 95%DMF	75	-0.84

Table 3.3 Peak potentials, E_p, and reductive charges, Q_{red}, obtained from cyclic voltammograms for the reduction of a monolayer in various incubation solutions.

References:

[3-1]: Troughton, E.B.; Batn, C.D.; Whitesides, G.M.; Nuzzo, R.G.; Allara, D.L.; Porter, M.D. *Langumir* **1988**, 4, 365.

[3-2]: Zhong, C.J.; Porter, M.D. *J. Am. Chem. Soc.* **1994**, 116, 11616.

[3-3]: Zhang, M.; Anderson, M.R. *Langmuir* **1994**, 10, 2807.

[3-4]: Hagenhoff, B.; Benninghoven, A.; Spinke, J.; Liley, L.; Knoll, W. *Langmuir* **1993**, 9, 1622.

[3-5]: Beulen, M.W.; Huisman, B.H.; van der Heijden, P.A.; van Veggel F.C.J.M.; Simons, M.G.; Biemond, E.M.E.F.; de Lange, P.J.; Reinhoudt, D.N. *Langmuir* **1996**, 12, 6170.

[3-6]: Biebuyck, H.A.; Bain, C.D.; Whitesides, G.M. *Langmuir* **1994**, 10, 1825.

[3-7]: Nuzzo, R.G.; Zegarski, B.R.; Dubois, L.H. *J. Am. Chem. Soc.* **1987**, 109, 773.

[3-8]: Porter, M.D.; Bright, T.B.; Allara, D.L.; Chidsey, C.E.D. *J. Am. Chem. Soc.* **1987**, 109, 3559.

[3-9]: Truong, K.D.; Rowntree, P.A. *J. Phys. Chem.* **1996**, 100, 19917.

[3-10]: Chuan-Jian Z.; Zak, K.; Porter, M.D. *J. Electroanal. Chem.* **1997**, 421, 9.

[3-11]: Snyder, R.G. *J. Chem. Phys.* **1967**, 47, 1316.

[3-12]: Widrig, C.A.; Chung, C.; Porter, M.D. *J. Electroanal. Chem.* **1991**, 310, 335.

[3-13]: Yang, D.F.; Wilde, C.P.; Morin, M. *Langmuir* **1996**, 12, 6570.

[3-14]: Yang, D.F.; Morin, M. *J. Electroanal. Chem.* **1997**, 429, 1.

[3-15]: Walczak, M.M.; Popenoe, D.D.; Deinhammer, R.S.; Lamb, B.D.; Porter, M.D. *Langmuir* **1991**, 7, 2687.

[3-16]: Hamelin, A. *Modern Aspects of Electrochemistry*; Conway, B.E.; White, R.E.; Bockris, J.O'M., Eds.; Plenum, New York, **1985**; Vol 16, Chapter 1.

[3-17]: Yang, D-F.; Lipkowski, J. *Langmuir* **1994**, 10, 2647.

[3-18]: Sondag-Huethorst, J.A.M.; Fokkink, L.G.J. *J. Electroanal. Chem.* **1994**, 367, 49.

[3-19]: Colthup, N.B.; Daly, L.H.; Widerley, S.E. *Introduction to infrared and Raman spectroscopy*, 3rd edition, Academic Press inc., SanDiego, **1990**.

[3-20]: Nuzzo, R.G.; Dubois, L.H.; Allara, D.L. *J. Am. Chem. Soc.* **1990**, 112, 558.

[3-21]: Ong, T.H.; Davies, P.B.; Bain, C.D. *Langmuir* **1993**, 9, 1836.

[3-22]: Lias, S.G.; Bartmess, J.E.; Leibman, J.F.; Holmes,J.L.; Levin, R.D.; Mallard, W.G. *J. of Physical and Chemical Reference Data* **1988**, 17, supplement No.1.

[3-23]: Schneider, T.W.; Buttry, D.A. *J. Am. Chem. Soc.* **1993**,115,12391.

Chapter 4

Mechanism of adsorption of sulfide on Au(111)

In this chapter, the electrochemical and vibrational properties of the alkanethiols, dialkyldisulfides and dialkylsulfides chemisorbed on a well-defined Au(111) single crystal substrate presented in the last chapter will be discussed. A mechanism of the oxidative dissociation of dialkylsulfide on a Au(111) single crystal surface will be presented.

4.1. Adsorption of symmetric dialkylsulfides on Au(111)

The results presented in the last chapter show that the vibrational spectra of the monolayers formed by long chain alkylsulfides are the same as monolayers formed by corresponding thiols. The wavelengths and widths of the C-H stretching bands for these monolayers are typical of alkanes in a crystalline state and their aliphatic chains have similar orientations.

The cyclic voltammograms of the reductive removal of the monolayer of sulfides and the corresponding thiols are identical. The cyclic voltammogram of didodecylsulfide in Fig 3.8 shows a reductive peak with an integrated charge of 107 $\mu C\ cm^{-2}$. When the potential is swept back, an oxidative redeposition peak appeared and it integrates for 70 $\mu C\ cm^{-2}$ (about 70% of the reductive charge). If we assume that the sulfide adsorbs molecularly and that the reductive process is a two-electron process, that is

$$R_2S\text{-}Au + 2e = RS^- + R^- + Au \qquad (4\text{-}1)$$

the surface coverage needs to be 1/2 of that of the thiols to give the same reductive charge. If the sulfide adsorbs molecularly on the Au(111) surface, when it readsorbs as a thiolate the oxidative charge should be lower than 50% of the reductive charge. This is not compatible with our results which show the oxidative charge to be as large as 70% of the reductive charge. Another result not compatible with the molecular adsorption of the sulfide is that when the monolayer formed by the dioctylsulfide is reduced in 0.1 M KOH, the integrated oxidative charge associated with the redeposition is only 18 $\mu C\ cm^{-2}$. However in 0.1 M $KClO_4$, this oxidative charge increases to 55 $\mu C\ cm^{-2}$. The larger fraction of the reduced molecules that is oxidatively redeposited in a solution of a lower pH can be explained by the lower solubility of thiols compared to that of thiolates. Insoluble compounds just remain at the surface and are thus redeposited more efficiently.

The results of chronoamperometric measurements of the reduction of the dibutylsulfides and the estimated sulfur coverages on gold for dialkylsulfides are similar to those of the corresponding alkane thiols[4-1 to 4-4]. Based on these results, we suggest that when a dialkylsulfide adsorb on a Au(111) surface, it forms a thiolate. Thus one of its C-S bonds is broken in the process of adsorption on the Au(111) surface.

4.2. Pentamethylene sulfide adsorption on Au(111)

Pentamethylene sulfide, the model molecule chosen to study the mechanism of sulfide adsorption on a gold surface, has allowed for the identification of the product of adsorption. The results show that the chemisorbed pentamethylene sulfides are oxidatively dissociated by molecular oxygen at the Au(111) surface.

We suggest the mechanism of the dissociation for pentamethylene sulfide at a Au(111) surface shown in the following equations. The first step is the adsorption of the sulfide on the gold surface (see eq.4-2). The sulfur would interact with the gold surface via its lone pairs of electrons. This stabilizing interaction between the sulfide and the Au(111) surface weakens the C-S bonds and makes the sulfur electron deficient. The second step is the attack of the carbon of the weakened C-S bond by molecular oxygen. The C-S bond is then broken homolytically. In the next step (see eq.4-4) the peroxo intermediate which is produced in step 2 (see eq.4-3) reacts with water (present in trace amount). In the last step of the reaction, a chemisorbed aldehyde-terminated thiolate and water are formed. The radicals •OH react with ethanol or with themselves.

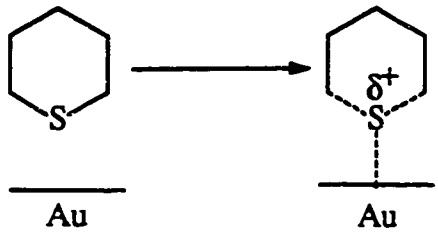

(4-2)

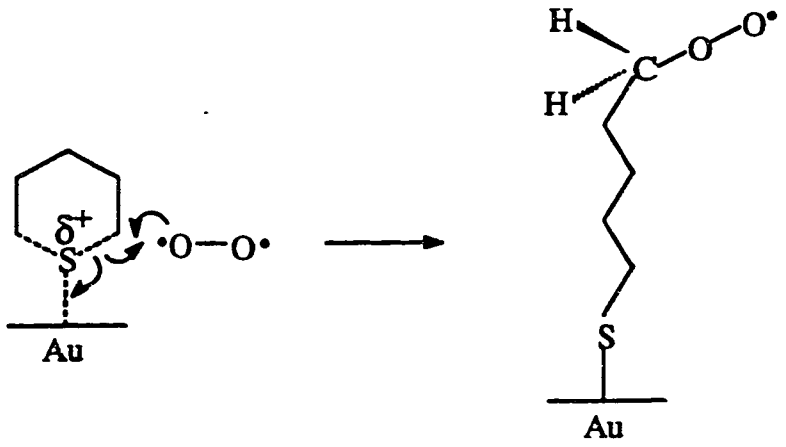

(4-3)

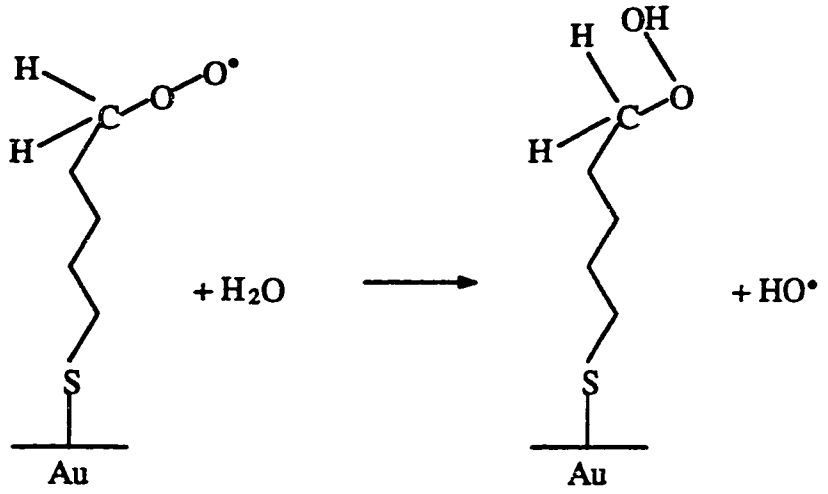

(4-4)

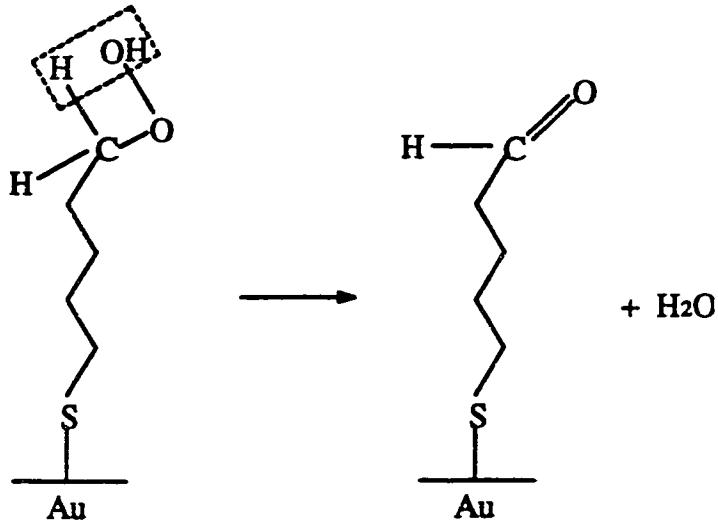

(4-5)

The mechanism for the oxidative dissociation of the pentamethylene sulfide should also occur for the dialkylsulfides, because the strengths of the C-S bond in both compounds are identical. The estimation[4-5,4-6,4-7] of the bond dissociation energy (BDE) of the C-S bond for the dialkanesulfide and the pentamethylene sulfide is as follows. Because the length of alkane chain does not affect the BDE of the C-S bond too much, we used C_2H_5-S-CH_3 to estimate the BDE of C-S bond for dialkanesulfide. $\Delta H_{f,CH3S^\bullet}$ = 31.4 kcal/mol, $\Delta H_{f,CH3CH2^\bullet}$ = 28 kcal/mol, $\Delta H_{f,C2H5SCH3}$ =

-14.2 kcal/mol so the BDE of C-S for $C_2H_5SCH_3$ = $\Delta H_{f,CH3CH2^\bullet}$ + $\Delta H_{f,CH3S^\bullet}$ - $\Delta H_{f,C2H5SCH3}$ = 73.6 kcal/mol = 308 kJ/mol. In the case of pentamethylene sulfide, we assume the two ends of the molecule $CH3(CH_2)_4SH$ do not affect each other and form a biradical $\bullet CH_2CH_2CH_2CH_2CH_2S\bullet$. The BDE of S-H for RS-H and RCH_2-H are 88.9 kcal/mol and 100 kcal/mol respectively, $\Delta H_{f,H^\bullet}$ = 52.1 kcal/mol, $\Delta H_{f,C5H11SH}$ = -26.23 kcal/mol, so $\Delta H_{f,\ \bullet CH2CH2CH2CH2CH2S\bullet}$ = BDE of S-H + BDE of C-H - $2\Delta H_{f,H^\bullet}$ - $\Delta H_{f,C5H11SH}$ = 58.47 kcal/mol, and $\Delta H_{f,pentamethylene\ sulfide}$ = -14.79 kcal/mol . The BDE in C-S for pentamethylene sulfide = $\Delta H_{f,\ \bullet CH2CH2CH2CH2CH2S\bullet}$ - $\Delta H_{f,pentamethylene\ sulfide}$ = 73.26 kcal/mol = 306 kJ/mol. We thus expect that the same activated species is formed upon adsorption of the dialkylsulfide and pentamethylene sulfide and that oxidative dissociation occurs. The mechanism of the oxidation of the dialkylsulfide by molecular oxygen to form an aldehyde is also compatible with the formation of an ordered monolayer since the aldehyde is soluble in ethanol.

4.3. S_N2 chemistry on the Au(111) surface

In order to confirm the formation of the reactive chemisorbed pentamethylene sulfide on the Au(111) surface as shown in eq.4-2, we use S_N2 chemistry. The four nucleophiles (ammonia, acetate, hydroxide and ethanolate), showed that different nucleophiles formed different functional groups of the chemisorbed thiolates on the gold surface. These results support the presence of an activated chemisorbed sulfide. We thus propose the following S_N2 mechanism:

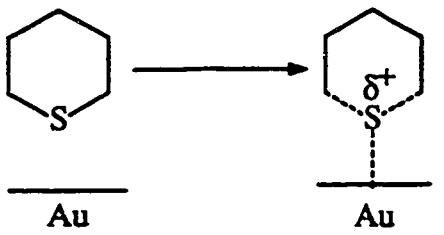

(4-6)

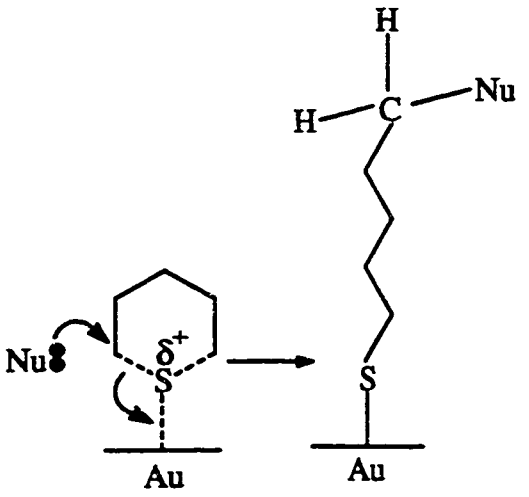

(4-7)

As we already discussed in the last section, the C-S bonds of the chemisorbed pentamethylene sulfide on gold are weakened because of the interaction of the sulfur with the gold surface via its lone electron pairs. Because of this interaction, the electron deficient sulfur becomes a good leaving group and thus a weaker nucleophile. This facilitates the nucleophilic substitution. The nucleophile, Nu: , attacks the carbon of the C-S bond as shown in eq. 4-7. The C-S bond breaks and a chemisorbed thiolate terminated by the nucleophile is formed as the final product.

Our conclusion that the sulfide was oxidatively dissociated when chemisorbed on Au(111) single crystal does not agree with the previous reports[4-8 to 4-11] of molecular adsorption of the sulfides. This difference is not due to the incubation medium because undegassed ethanolic solutions of the sulfide were used by all. The difference is likely to originate from the different gold substrates used. Others used gold films deposited on a glass or silicon substrate, while we used a Au(111) single

crystal. So we conclude that the structure of the gold surface plays a role in the dissociation of the sulfide. The heterogeneity of adsorption sites (i.e., steps, defects, vacancies and terraces) on gold films deposited on glass or silicon could lead to dissociative and/or molecular adsorption of a sulfide. It is possible that on specific adsorption sites the C-S bond is not weakened enough for the oxidation of the sulfide by molecular oxygen to proceed, but on other adsorption sites dissociation of the sulfide may be possible.

The oxidative dissociation of sulfides suggests that a similar process might occur for the thiols. The BDE of the S-H bond is about 370 kJ/mol[4-5,4-7], a value higher than the BDE of S-C bond. The two adsorption mechanisms of thiols suggested previously are:

$$2\,RS\text{-}H + Au \rightarrow 2\,RS\text{-}Au + H_2 \qquad (4\text{-}8)$$

$$2\,RS\text{-}H + Au + Oxidant \rightarrow 2\,RS\text{-}Au + H_2O \qquad (4\text{-}9)$$

We believe the first step of the adsorption of thiols should be the formation of activated (or weakened) chemisorbed thiols on the gold surface. Since the S-H bond is strong, the process shown in eq.4-8 should be difficult. Once the S-H bond is broken, a Au-H should be formed. There is no evidence of hydrogen adsorbed on gold[4-12]. Finally, two hydrogens must diffuse close to one another and combine to give H_2. We thus believe the formation of an actived chemisorbed thiol followed by its oxidation (eq.4-9) is most likely to occur on the Au(111) surface.

References:

[4-1]: Widrig, C.A.; Chung, C.; Porter, M.D. *J. Electroanal. Chem.* **1991**, 310, 335.

[4-2]: Yang, D.F.; Wilde, C.P.; Morin, M. *Langmuir* **1996**, 12, 6570.

[4-3]: Yang, D.F.; Morin, M. *J. Electroanal. Chem.* **1997**, 429, 1.

[4-4]: Walczak, M.M.; Popenoe, D.D.; Deinhammer, R.S.; Lamb, B.D.; Porter, M.D. *Langmuir* **1991**, 7, 2687.

[4-5]: Lias, S.G.; Bartmess, J.E.; Leibman, J.F.; Holmes,J.L.; Levin, R.D.; Mallard, W.G. *J. of Physical and Chemical Reference Data* **1988**, 17, supplement No.1.

[4-6]: Moran, S.; Ellison, G.B. *J. Phys. Chem.* **1988**, 92, 1794.

[4-7]: Benson, S.W. *Thermochemical Kinetics, methods for the estimation of thermochemical data and rate parameters, 2nd Editon.* A wiley-interscience Publication John Wiley & Sons, New York, **1976.**

[4-8]: Troughton, E.B.; Batn, C.D.; Whitesides, G.M.; Nuzzo, R.G.; Allara, D.L.; Porter, M.D. *Langumir* **1988**, 4, 365.

[4-9]: Zhang, M.; Anderson, M.R. *Langmuir* **1994**, 10, 2807.

[4-10]: Hagenhoff, B.; Benninghoven, A.; Spinke, J.; Liley, L.; Knoll, W. *Langmuir* **1993**, 9, 1622.

[4-11]: Beulen, M.W.; Huisman, B.H.; van der Heijden, P.A.; van Veggel F.C.J.M.; Simons, M.G.; Biemond, E.M.E.F.; de Lange, P.J.; Reinhoudt, D.N. *Langmuir* **1996**, 12, 6170.

[4-12]: Ulman, A. *An introduction to ultrathin organic films from Langmuir-Blodgett to self-assembly*, Academic Press; Boston, **1991**.

Chapter 5

Conclusion

The electrochemical and spectroscopic properties of different alkanethiols, dialkyldisulfides and alkylsulfides adsorbed on the Au(111) surface have been measured. We found that all the thiols, disulfides and sulfides form monolayers with the same final product, a thiolate. The S-H bond of thiols, the S-S bond of disulfides and the S-C bond of sulfides are broken upon adsorption on the gold surface. The adsorption of sulfides is complex. The surface chemistry of the sulfide was influenced by the structure of the substrate and the chemical species in the incubation medium.

Using a cyclic sulfide - pentamethylene sulfide, we studied the mechanism of adsorption of sulfides on a Au(111) single crystal. This produces an aldehyde and a chemisorbed thiolate.

Four different nucleophiles (ammonia, acetate, hydroxyl and ethanolate) were added to the pentamethylene sulfide incubation solution and S_N2 reactions occurred. This proved that the sulfide chemisorbed on the gold surface is reactive, because it can react with the weak nucleophile, NH_3. However, it was stable enough not to react with water, a weaker nucleophile.

IMAGE EVALUATION TEST TARGET (QA-3)

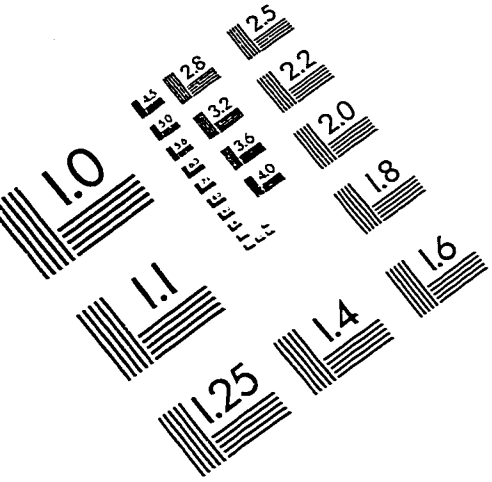

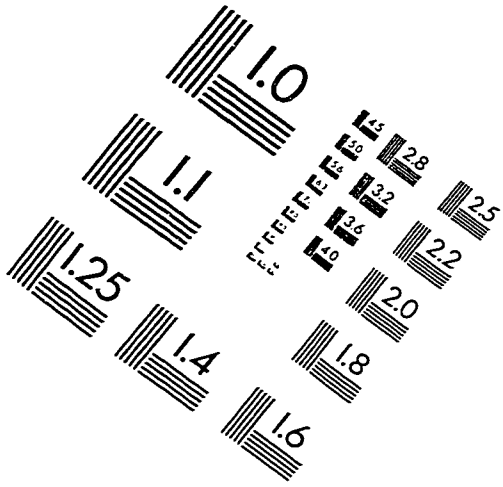

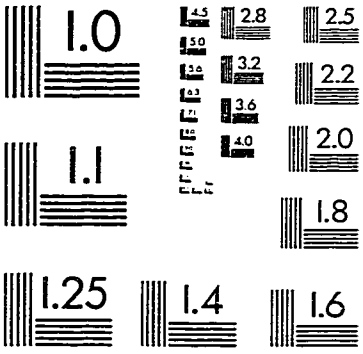

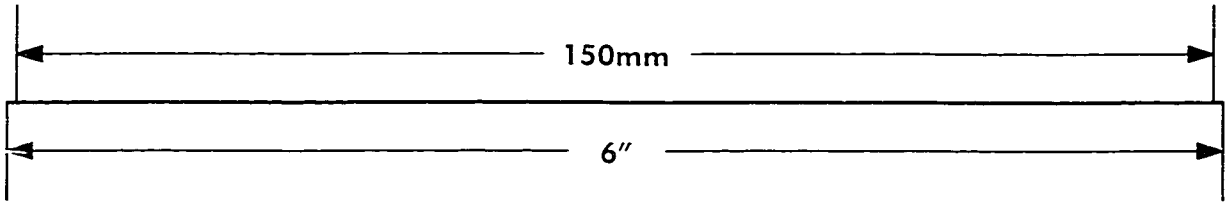

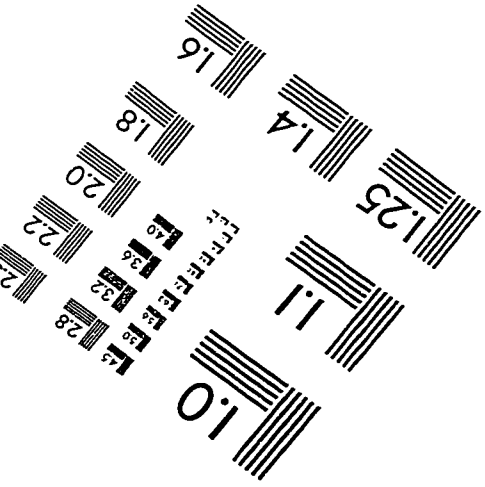

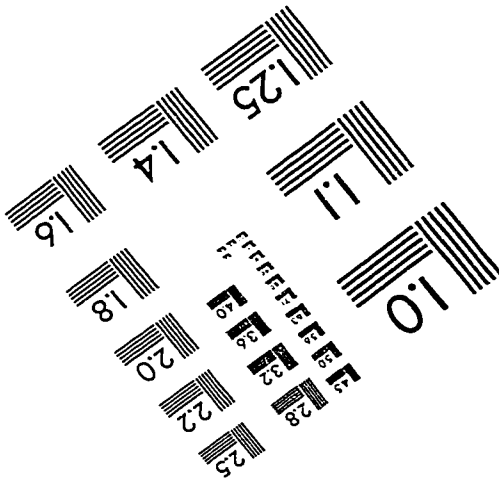

APPLIED IMAGE, Inc
1653 East Main Street
Rochester, NY 14609 USA
Phone: 716/482-0300
Fax: 716/288-5989